Electrogenic reactions in the heme-copper oxidase family of enzymes

Audrius Jasaitis

Institute of Biotechnology and
Department of Biosciences,
Division of Biochemistry,
Faculty of Sciences
University of Helsinki

Academic dissertation
To be presented for public criticism, with permission of the Faculty of Science, University of Helsinki, in the auditorium 1041 of the Biocenter 2 (Viikinkaari 5) on February 21st, 2002, at 12 o'clock noon

Supervisors: Professor Michael Verkhovsky
Institute of Biotechnology
University of Helsinki, Finland

Professor Mårten Wikström
Institute of Biotechnology
University of Helsinki, Finland

Reviewers: Professor Ilmo Hassinen
Department of Medical Biochemistry
Faculty of Medicine
University of Oulu, Finland

Professor Robert Gennis,
University of Illinois at Urbana-Champaign
U.S.A.

Opponent: Professor Peter Brzezinski
Department of Biochemistry
Arrhenius Laboratories for Natural Sciences
Stockholm University, Sweden

ISSN 1239-9469
ISBN 952-91-0294-8 (nid.)
ISBN 952-91-0295-6 (pdf, http://ethesis.helsinki.fi)
Yliopistopaino
Helsinki 2002

List of original publications

I. **Jasaitis, A**., Verkhovsky, M.I., Morgan, J.E., Verkhovskaya, M.L., and Wikström, M. Assignment and charge translocation stoichiometries of the major electrogenic phases in the reaction of cytochrome *c* oxidase with dioxygen (1999) *Biochemistry* **38**, 2697-2706.

II. **Jasaitis, A**., Borisov, V., Belevich, N., Morgan, J.E., Konstantinov, A.A. and Verkhovsky, M.I. Electrogenic reactions in cytochrome *bd* oxidase (2000) *Biochemistry* **39**, 13800-13809

III. **Jasaitis, A.**, Backgren, C., Verkhovsky, M.I., Puustinen, A., and Wikström, M. Electron and Proton Transfer in the Arginine-54-Methionine Mutant of Cytochrome *c* Oxidase from *Paracoccus denitrificans* (2001) *Biochemistry* 40, 5269-5274

IV. Verkhovsky, M.I., **Jasaitis, A.**, Verkhovskaya, M.L., Morgan, J.E., and Wikström, M. Proton translocation by cytochrome *c* oxidase. (1999) *Nature* 400, 480-483.

V. Verkhovsky, M.I., **Jasaitis, A.**, and Wikström, M. Ultrafast heme-heme electron transfer in cytochrome *c* oxidase (2001) *Biochim. Biophys Acta* 1506, 143-146.

Abbreviations and Symbols

A – ferrous-oxy intermediate

ATP – adenosine triphosphate

BTP – 1,3-bis(tris(hydroxymethyl)methylamine)propane

$\Delta\psi$ – electric potential

$\Delta\tilde{\mu}_{H^+}$ – electrochemical proton gradient

d – dielectric depth of the hemes in the membrane

DCPIP – dichlorophenolindophenol

E_h – redox midpoint potential

F – ferryl-oxo intermediate

H – high potential oxygen intermediate

MV – mixed-valence state of the binuclear site

N-side – negatively charged side of the membrane

NADH – reduced nicotinamide adenine dinucleotide

O – fully oxidized form of binuclear oxygen reduction site

P – peroxy oxygen intermediate

P-side – positively charged side of the membrane

R – unliganded, fully reduced form of the binuclear site

RT – room temperature

Rubipy – tris(2,2'-bipyridyl)ruthenium (II)

Su – subunit

TMPD – N,N,N',N'-tetramethyl-1,4-phenylenediamine

1. Introduction

1.1 Energy cycle in living organisms

Sunshine is the only external source of energy on Earth. During evolution, plants and some bacteria acquired the ability to utilize the energy of light from the Sun. Photosynthesis is a very complicated process during which molecules of water and carbon dioxide are combined to form energy-rich molecules. As a consequence, the energy of the photon is converted and stored in the energy of chemical bonds. Later during evolution, organisms appeared which were able to use energy-rich substances as a source of food and use that stored energy for their own needs. In these organisms, as a result of metabolism, oxygen is consumed and water and carbon dioxide are formed. This later process is called respiration. Taken together, photosynthesis and respiration make a closed energy cycle:

$$6CO_2 + 6H_2O \underset{Respiration}{\overset{Photosynthesis}{\rightleftharpoons}} C_6H_{12}O_6 + 6O_2$$

1.2 Respiration

In the cells of higher organisms the energy production is localized in small organelles called mitochondria. Mitochondria consist of two closed layers of membrane, identified simply as the outer and inner membrane. The outer membrane is smooth and delineates the size of the organelle. The area of the inner membrane is very large. The inner membrane projects into the interior space of the mitochondria, to form the so-called cristae, which greatly enhance the surface area of this membrane. The inner membrane contains many enzymatic complexes, which are specialized in energy conservation. Prokaryotes do not contain mitochondria. In these organisms the energy conserving enzymes are located in the cytoplasmic membrane. In both higher organisms and aerobic bacteria the energy conservation primarily occurs through the process called oxidative phosphorylation. During this process electrons are passed along a series of transmembrane enzymatic complexes, which together form an electron transport chain. Energy is conserved in a form of an electrochemical transmembrane proton gradient, which is subsequently used for ATP synthesis.

Reduced nicotinamide adenine dinucleotide (NADH) is the first electron donor in the mitochondrial electron transport chain (Fig. 1). NADH is produced by the oxidation of nutrients such as different sugars, fats and proteins. Electrons enter the electron transport chain through the NADH dehydrogenase. It is a very large and complex transmembrane protein which contains variety of redox cofactors. This enzyme, which is also called Complex I, donates electrons to the quinone pool in the membrane. The reduced quinone pool is also maintained by the membrane bound dehydrogenases, for example succinate dehydrogenase (Complex II; Fig. 1). The bc_1 complex, or Complex III, oxidizes the reduced quinone pool and passes electrons to water soluble cytochrome *c*. The final acceptor of electrons in the respiratory chain is the oxygen molecule and the enzyme that catalyses the reduction of oxygen is cytochrome *c* oxidase or Complex IV. It transfers electrons from cytochrome *c* to the bound oxygen and reduces it to water.

In addition to the transfer of electrons from energy rich foodstuff, Complexes I, III and IV also transfer protons across the mitochondrial membrane. This creates an electric potential ($\Delta\psi$) and a proton concentration difference across the membrane (ΔpH), which combines to form the so-called electrochemical proton gradient ($\Delta\tilde{\mu}_{H^+}$). The electrochemical proton gradient

across the membrane is used by ATP synthase to drive the ATP synthesis from ADP and inorganic phosphate. This process was first described by Peter Mitchell in his chemiosmotic theory (Mitchell, 1961).

Cytochrome *c* oxidase is the terminal enzyme in the respiratory chain of mitochondria and aerobic bacteria. This enzyme ultimately couples the electron transfer from cytochrome *c* to the oxygen molecule with proton translocation across the inner mitochondrial membrane (Wikström, 1977). This reaction requires complicated chemical processes to occur at the catalytic site of the enzyme in coordination with proton translocation, the exact mechanism of which is not known at the present. The mechanisms underlying the fast reactions of cytochrome *c* oxidase; oxygen activation, electron transfer and coupling of electron transfer to proton

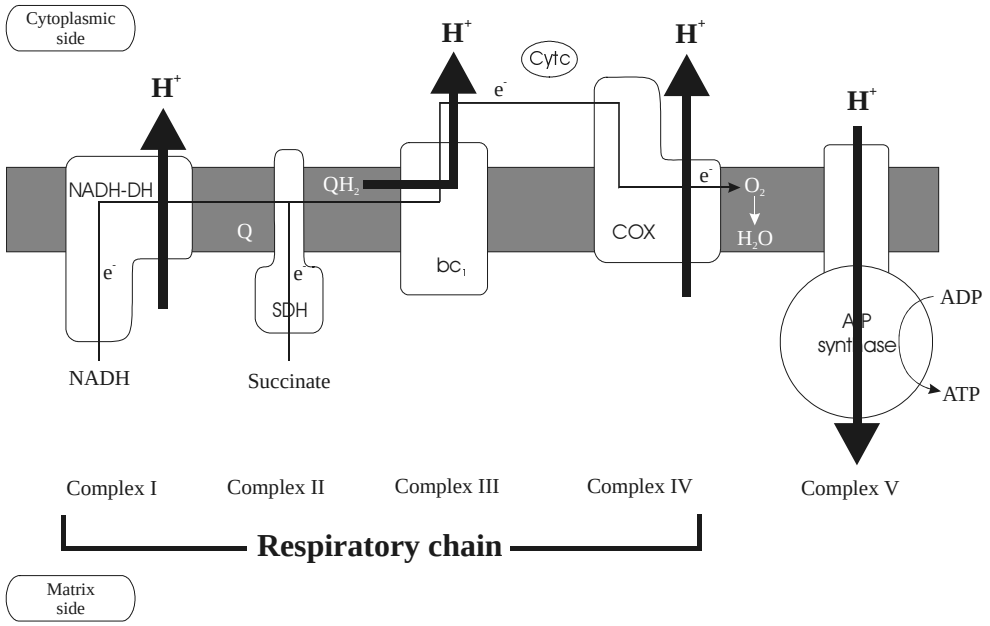

Figure 1. A simplified view of the mitochondrial electron transport chain

translocation are the main questions in the field of bioenergetics.

2. Review of the literature

2.1 Function

Cytochrome *c* oxidase accepts electrons from reduced cytochrome *c* and catalyses the reduction of dioxygen to two water molecules:

$$O_2 + 4H^+ + 4e^- \rightarrow 2H_2O$$

This reaction has a very high activation barrier and does not occur spontaneously under normal conditions. On the other hand, the reduction of oxygen is highly exergonic and large amounts of energy are released during this process. The function of cytochrome *c* oxidase is to activate the oxygen molecule and to conserve the energy released during this reaction. The energy is conserved in the form of an electrochemical proton gradient across the membrane ($\Delta\tilde{\mu}_{H^+}$). There are two principles by which cytochrome *c* oxidase generates $\Delta\tilde{\mu}_{H^+}$ – vectorial chemistry and proton pumping. The first principle is a direct consequence of the oriented chemistry inside the protein. Natively, the enzyme is in the lipid membrane of mitochondria or a prokaryotic cell where electrons enter the enzyme from cytochrome *c* from one side of the membrane and the protons required to make water are taken from the other side of the membrane. Only chemical processes contribute to the transfer of four charges across the lipid membrane. In addition, cytochrome *c* oxidase is a proton pump (Wikström, 1977). For each molecule of oxygen reduced during the catalytic cycle the enzyme transfers four protons across the membrane. The overall reaction of the terminal oxidases can therefore be summarized by the equation:

$$O_2 + 8H_i^+ + 4e^- \longrightarrow 2H_2O + 4H_o^+$$

where H_i^+ – protons taken-up from the **N**-side and H_o^+ – protons released to the **P**-side of the membrane.

The other aspect of the function of cytochrome *c* oxidase is to assure complete reduction of dioxygen to water. There are several highly reactive intermediate oxygen species, such as superoxide, peroxide and various radicals, which are formed by partial reduction of the oxygen molecule. All those species can cause damage inside the cell and also damage the enzyme itself. Cytochrome *c* oxidase keeps these reactive oxygen species bound inside the protein during the process of reduction thus guaranteeing the safety of itself and the mitochondria in general.

2.2 Structure and spectroscopic properties of cytochrome *c* oxidase

2.2.1 The family of the heme–copper oxidases

Cytochrome *c* oxidase is a member of the large family of enzymes known as heme-copper oxidases. It has long been recognized that bacterial respiratory systems are branched, having a number of distinct terminal oxidases, rather than the single cytochrome *c* oxidase as is present in most eucaryotic mitochondrial systems. There are more than 80 known members of this group (Garcia-Horsman *et al.*, 1994). The family of heme-copper oxidases has one main feature in common. This feature is six fully conserved histidine residues in subunit I, which ligate the redox active metal centers and a unique binuclear heme iron–copper, oxygen reduction

center. In bacteria, the heme groups can be hemes A, B, C or O (Calhoun *et al.*, 1994), whereas only heme A is found in mitochondrial cytochrome *c* oxidases.

There are two groups of heme-copper oxidases, which differ by the nature of the electron donor. Cytochrome *c* oxidases accept electrons from the water soluble cytochrome *c*. The best known and the most studied members of this group are the mitochondrial cytochrome *c* oxidase and cytochrome *c* oxidases from *Paracoccus denitrificans* and *Rhodobacter sphaeroides*, also known as cytochrome aa_3. The other group are the quinol oxidases. These oxidases accept electrons from membrane soluble quinols. This class is often represented by cytochrome bo_3 from *Escherichia coli*.

The members of the heme-copper oxidase family are electrogenic proton pumps (Wikström, 1977; Garcia-Horsman *et al.*, 1994). For each oxygen molecule reduced, the enzyme transfers four additional protons across the membrane. There is also an entirely different class of terminal oxidases, widely distributed in the bacterial kingdom but represented so far by a single member, a quinol oxidase of the *bd* type. In *E. coli*, cytochrome *bd* is one of two terminal quinol oxidases and this enzyme have been characterized in significant detail (Junemann, 1997). It has been demonstrated that this class of enzymes consumes oxygen in a similar way to the heme-copper oxidases but does not pump protons (Puustinen *et al.*, 1991). In contrast to heme-copper oxidases, cytochrome *bd* contains no copper, but has three hemes: heme b_{558}, which has a relatively low midpoint potential, and hemes b_{595} and *d*. The latter two hemes are both high potential and form a heme-heme reaction center, reminiscent of the heme-copper binuclear site in the heme-copper oxidase family.

2.2.2 Major subunits

As a consequence of their central position in metabolism, the cytochrome *c* oxidases have been intensively studied using biochemical, genetic, spectroscopic and crystallographic methods. All the major aspects and key residues of the structure of the cytochrome *c* oxidase are known from mutagenesis studies. Nearly all conserved residues of subunit I have been mutated in the bacterial cytochrome *c* oxidases and the mutant enzymes have been characterized (Hosler *et al.*, 1993). Recently, the high-resolution structures of cytochrome *c* oxidase from bovine heart (Tsukihara *et al.*, 1996), cytochrome aa_3 from *P. denitrificans* (Iwata *et al.*, 1995), cytochrome ba_3 from *Thermus thermophilus* (Soulimane *et al.*, 2000) and cytochrome bo_3 from *E. coli* (Abramson *et al.*, 2000) have been solved using X-ray crystallographic data.

The mammalian cytochrome *c* oxidase contains 13 subunits, 3 of which are encoded within the mitochondrial genome (subunits I, II and III) with the remaining 10 being encoded by the nuclear genome (Capaldi, 1990). Nearly all of the bacterial oxidases contain homologs of subunits II and III in addition to subunit I. Homologs of the 10 nuclear-encoded subunits of the mammalian oxidases have not been found in bacteria. The cytochrome *c* oxidase from *P. denitrificans* consists of the three core subunits I, II, and III and a small non-conserved subunit IV of unknown function (Witt and Ludwig, 1997). The structure of the bacterial and the mitochondrial enzymes are surprisingly similar. The core parts (subunits I, II and III) of the two crystal structures are nearly identical at the atomic level. All active sites of cytochrome *c* oxidase are contained in subunits I and II.

Subunit I is the largest and best-conserved subunit of cytochrome *c* oxidase. It contains 12 transmembrane helices and if viewed from the top of the membrane the helices are arranged in an anticlockwise sequential manner and appear to form three symmetry-related semicircular arcs consisting of four helices each (Michel *et al.*, 1998). Subunit I contains the two heme groups: heme *a* and heme a_3. Heme a_3 together with a copper atom (Cu_B) forms the binuclear center that is the catalytic site for oxygen reduction. Both hemes are buried in the enzyme about

15 Å from the P-side of the membrane. The heme planes are perpendicular to the membrane surface and the two propionate groups of each heme point toward the P-side of the membrane. The heme groups approach each other edge-to-edge at a minimal distance of 7.3 Å and form an interplanar angle of 104° in the *P. denitrificans* structure (Michel *et al.*, 1998).

Heme a_3 is considered to be high-spin both in the resting ferric state (S=5/2) and the fully reduced ferrous state (S=2). In the electron density map of the crystal structure the iron appears to be five-coordinated. Four nitrogen atoms of a porphyrin ring ligate the heme iron and a conserved histidine imidazole of helix X (Su I-His 411) is the axial, fifth ligand. The hydroxyethylfarnesyl group of heme a_3 penetrates into the lipid bilayer so that access of protons to the binuclear center is principally possible from the P-side of the membrane.

For the heme structure in general, the 0-0 $\pi \rightarrow \pi^*$ transition leads to an intense absorbance band in the Soret region between 400-450 nm and a less intense band in the visible region, the alpha band, centered around 600 nm (Platt, 1956). The reduced-minus-oxidized absorbance spectrum of heme a_3 has a characteristic high-intensity absorbance band with a maximum at 445 nm and minimum at 414 nm in the Soret spectral region. The absorbance in the alpha spectral region for heme a_3 is much less pronounced than the Soret band with a split maximum absorbance band at 588 nm and 609 nm (Hellwig *et al.*, 1999). A weaker secondary band, the beta band, is observed at ~560 nm in the visible region and is due to a 0-1 vibronic transition. In addition to the $\pi \rightarrow \pi^*$ transitions, the fully oxidized enzyme shows a weak band at ~660 nm due to the high-spin ferric heme a_3 (Beinert *et al.*, 1976; Carter and Palmer, 1982). This band has been postulated to be due to charge-transfer to the ligand of heme a_3 (Mitchell *et al.*, 1991) and to be modulated by the redox state of Cu_B (Beinert *et al.*, 1976).

The Cu_B atom is 4.5 Å away from the heme a_3 iron. Together heme a_3 and Cu_B form a binuclear oxygen reduction center. Cu_B has three histidine imidazole ligands (Su I-His 276, Su I-His 325 and Su I-His 326). A combination of EXAFS and ENDOR spectroscopy suggests a fourth ligand, most likely a water or a hydroxide ion, in the oxidized enzyme (Fann *et al.*, 1995). A possible bridging structure is a hydroxide ion bound to Cu_B and hydrogen-bonded to a water ligand of the heme a_3 iron. The absorbance changes of Cu_B associated with the redox events during turnover of the enzyme have yet to be detected and assigned. Cu_B and heme a_3 are so close that they electronically influence each other. Therefore, Cu_B is usually invisible, also to EPR spectroscopy. There are only a few exceptional cases where it was possible to detect an EPR signal arising from Cu_B (Karlsson and Andréasson, 1981; Hansson *et al.*, 1982; Blair *et al.*, 1985; Morgan *et al.*, 2001). In all these cases, the shape of the signal was the same – four peaks centered around g=2.26, but exhibited different saturation conditions depending on the preparation of the sample.

Heme *a* is a low spin, six-coordinated heme in both the oxidized (S=1/2) and reduced (S=0) forms of the enzyme as demonstrated by MCD and resonance Raman spectroscopy (Babcock *et al.*, 1976; Babcock *et al.*, 1981; Carter and Palmer, 1982; Eglinton *et al.*, 1984). In addition to the four ligands from the porphyrin ring, it is ligated by two very well conserved histidine imidazoles of helices II and X (Su I-His 94, Su I-His 413) as axial Fe ligands. The latter histidine is two residues upstream from the heme a_3 histidine ligand. In contrast to heme a_3 its hydroxyethylfarnesyl side chain points to the N-side of the membrane. Together with the surrounding hydrophobic residues the sidechain blocks access to heme *a* from the N-side of the membrane.

The reduced-minus-oxidized spectrum of heme *a* has a characteristic absorption maximum at 445 nm and minimum at 430 nm in the Soret region and maximum at 605 nm in the alpha region. The extinction coefficient of the absorbance bands in the Soret region are smaller compared to heme a_3, but in the alpha region heme *a* absorbs much more intensively and the absorbance band is much sharper than that of heme a_3. The peak positions of the absorbance spectrum of heme *a* are very unusual for the low spin A-type heme: they are significantly red

shifted. The formyl group of heme *a* forms a strong hydrogen bond with the Su I-Arg 54. This interaction strongly affects the optical spectrum of the heme (Kannt *et al.*, 1999; Riistama *et al.*, 2000).

Subunit II of the cytochrome *c* oxidase from *P. denitrificans* consists of two transmembrane helices interacting with subunit I and a large C-terminal extramembranous domain containing one more redox center - Cu_A. Cu_A is located above subunit I in the periplasmic or intermembrane space. The structure of the extramembranous domain has also been determined using a quinol oxidase fragment containing an engineered copper center (Wilmanns *et al.*, 1995). The binding site for the two copper atoms is formed by residues from β-sheet 6 and the loop connecting β-sheets 9 and 10. The ligands for each Cu atom form a distorted tetrahedron. Two Cys residues and one His residue ligate both Cu atoms. Each Cu atom has an additional ligand: in one case a methionine and in the other the carbonyl oxygen of a glutamate residue. The two copper atoms are bridged by the two cysteine thiolates, and the copper atoms and Cys sulfurs lie in one plane.

Cu_A is a diatomic site. Recent evidence suggests that both copper atoms in the oxidized state are in a mixed valence [Cu(1.5)-Cu(1.5)] configuration (Antholine *et al.*, 1992; van der Oost *et al.*, 1992; Kelly *et al.*, 1993; Lappalainen *et al.*, 1993; Malmström and Aasa, 1993; Steffens *et al.*, 1993). The optical absorbance spectrum of the Cu_A site was determined using the specially prepared soluble Cu_A binding domain (subunit II) from the *P. denitrificans* cytochrome *c* oxidase (Lappalainen *et al.*, 1993). Using the soluble form of subunit II, Cu_A exhibits a very broad absorbance band in the region of 830 nm with a small extinction coefficient and more intense absorbance bands in the region of 500 nm. The absorbance band at 830 nm is characteristic for Cu_A because this spectral region does not overlap with the absorbance of the hemes.

Bacterial oxidases are significantly simpler in composition, containing three subunits with strong homology to subunits I, II and III of eukaryotes. Some bacterial oxidases contain heme A as a prosthetic group and cytochrome *c* as a substrate, but in others heme A has been replaced by a different heme. For example, in cytochrome ba_3 from *Thermus thermophilus*, the low-spin heme *a* has been replaced by a protoheme but both Cu_A and Cu_B are still present (Zimmermann *et al.*, 1988). In cytochrome bo_3 from *E. coli* the heme at the binuclear site is heme O, which has the same structure as heme A except for a methyl group in place of the formyl group (Puustinen and Wikström, 1991; Wu *et al.*, 1992). In this enzyme, as well as cytochrome aa_3-600 from *Bacillus subtilis* and cytochrome aa_3 from *Sulfolobus acidocaldarius* (Lübben *et al.*, 1992), the electron donor is ubiquinol rather than cytochrome *c* and these enzymes lack Cu_A. *Rhodobacter capsulatus* (Gray *et al.*, 1994) and *Rhodobacter sphaeroides* (Garcia-Horsman *et al.*, 1994) have recently been shown to contain an alternative cbb_3-type cytochrome *c* oxidase, which contains a high-spin heme B at the binuclear center. This oxidase contains Cu_B but lacks Cu_A. A similar, if not identical enzyme in *P. denitrificans* pumps protons (Raitio and Wikström, 1994), indicating that the farnesyl side chain may not have a role in proton translocation as previously suggested (Woodruff *et al.*, 1991). Therefore, the common feature of the heme-copper oxidases is a binuclear center located in subunit I, containing a high-spin heme and Cu_B. Furthermore, all are able to function as redox-linked proton pumps, suggesting that the binuclear center is the site of the proton pump.

The cytochrome *c* oxidase – at least from mitochondria, *Rhodobacter sphaeroides*, and *P. denitrificans* – contain a non-redox-active Mn/Mg-binding site. In mitochondrial cytochrome *c* oxidase a Mg atom occupies this site. In bacteria, Mg is typically found in this site, however some species incorporate a substantial amount of manganese into this site when grown under Mg-limited conditions. This Mn/Mg binding site is located at the interface between subunits I and II. The Mg ion is ligated by Su I-His 403, Su I-Asp 404, Su II-Glu 218, and at least one water (Tsukihara *et al.*, 1996; Ostermeier *et al.*, 1997). An interesting feature is the arrangement

of the carbonyl oxygen from Su II-Glu 218 which is also a Cu_A ligand and of Su I-His 403 being hydrogen bonded to one of the heme a_3 propionates. Therefore, the Mg site lies directly between Cu_A and heme a_3. The function of the bound metal is not known.

Another metal binding site is reported in the crystal structures of cytochrome *c* oxidase from *P. denitrificans* (Ostermeier *et al.*, 1997) and bovine heart mitochondria (Yoshikawa *et al.*, 1998). This site, which was proposed to bind either Ca^{2+} or Na^+ (Ostermeier *et al.*, 1997; Yoshikawa *et al.*, 1998), is situated on the P-side membrane border of subunit I, and appears well accessible as it is not blocked by the other subunits. The identity of the ion cannot be determined from the presently available crystal structures. In *P. denitrificans*, the authors prefer coordination with Ca^{2+} whereas Na^+ is preferred in the structure proposed by Yoshikawa. The binding of both Ca^{2+} and Na^+ causes a shift of the absorption spectra of heme *a* in the enzyme (Riistama *et al.*, 1999), which is similar to the red-shift of the heme *a* spectrum upon "energization" of isolated mitochondria by ATP (Wikström and Saris, 1970; Wikström, 1972; Wilks and Ortiz de Montellano, 1992).

2.2.3 Additional subunits.

The bacterial cytochrome *c* oxidases have only one additional subunit in some instances (Su IV). The X-ray structural analysis of *P. denitrificans* cytochrome aa_3 revealed that the fourth subunit consists mainly of one transmembrane helix interacting with subunits I and III (Iwata *et al.*, 1995). The function of this fourth subunit is unknown. The deletion of the gene encoding this subunit has no obvious effect on bacterial growth, expression of the mutant protein, or the enzymatic properties of the purified enzyme (Witt and Ludwig, 1997).

The mammalian cytochrome *c* oxidase from bovine heart has ten additional subunits. Again their function is unknown. The subunits Va and Vb are small globular proteins bound to the matrix side of the core subunits and the globular subunit VIb faces the intermembrane space. Subunit VIb binds zinc ion, of unknown function, in a tetrahedral coordination. The subunits IV, VIa, VIc, VIIa, VIIb, VIIc and VIII each possess one transmembrane helix. Subunit VIa seems to be responsible for the dimmerization of the mitochondrial cytochrome *c* oxidase (Tsukihara *et al.*, 1996). It has been suggested that the small subunits act as regulators and bind effectors of enzyme activity such as nucleotides (Kadenbach, 1986) or are required for assembly. Tsukihara *et al*. (1996) found two cholate-binding sites in the crystal structure and proposed them to be potential nucleotide binding sites. The presence of tissue specific isoforms of several additional subunits supports the hypothesis of a regulatory function (Kuhn-Neutwig and Kadenbach, 1985; Yanamura *et al.*, 1988).

2.3 Electron transfer pathways and kinetics in cytochrome *c* oxidase

Numerous kinetic measurements on cytochrome *c* oxidase have been aimed at determining the electron transfer rates between the redox centers. The elucidation of the electron transfer pathways from cytochrome *c* to the binuclear site is clearly relevant to the mechanism by which these processes may be coupled to proton pumping.

While most of the early steady-state and stopped-flow experiments favored heme *a* over Cu_A as the primary acceptor of electrons from cytochrome *c* *in vivo* (reviewed by Brunori (1988)), more recent transient kinetic studies suggest the opposite. Now Cu_A is generally accepted as being the primary electron acceptor from cytochrome *c* (Hill, 1991). The electron transfer rate between cytochrome *c* and Cu_A is very fast, about 60000-70000 s^{-1} (Hill, 1994; Geren *et al.*, 1995). The electron transfer is a very fast event and it has been proposed that the

formation of the complex between cytochrome *c* and cytochrome *c* oxidase is the rate-limiting step in the reaction between reduced cytochrome *c* and the oxidase (Antalis and Palmer, 1982). The nature of the binding interaction is still unclear. The strong dependence on ionic strength is indicative of electrostatic interactions stabilizing the complex (Rieder and Bosshard, 1980; Antalis and Palmer, 1982).

From Cu_A electrons are transferred to heme *a* at a relatively high speed (about 20000 s^{-1}) considering the long metal-to-metal distance (19.5 Å) and small driving force of 50 mV (Winkler *et al.*, 1995). The crystal structure shows that the distances from Cu_A to the iron atoms of heme *a* and heme a_3 are 19.5 Å and 22.1 Å respectively. Surprisingly only the electron pathway *via* heme *a* is used in cytochrome *c* oxidase.

From heme *a* the electron is transferred to heme a_3. As mentioned previously, these hemes are nearly perpendicular to each other. While the iron-to-iron distance is 13.5 Å (Michel *et al.*, 1998) the edges of the hemes approach each other up to 7.3 Å. An edge-to-edge electron transfer is therefore possible as well as a pathway using the iron ligands Su I-His 413 and Su I-His 411 and the polypeptide backbone.

There are at least two theoretical models to describe electron transfer in proteins. In one, biological electron transfer is considered to occur along specific pathways in the structure (Gray and Winkler, 1996), which allows structural control of the electron transfer rate. The other is an empirical theory of nonadiabatic electron transfer (Moser *et al.*, 1992; Page *et al.*, 1999) in which the electron tunneling rate between biological cofactors is determined by the edge-to-edge distance between them, and by the atomic packing density of the intervening structure. In the second model it is thought that electron transfer is possible through a large number of pathways, and is not limited to one or a few pathways that might have specifically evolved for the purpose. Compilation of data from many proteins seems to agree with the latter concept (Page *et al.*, 1999). Both theories of electron transfer in proteins have their advantages and drawbacks and neither has been unequivocally accepted in the field.

There is another experimental approach available to study the electron transfer processes in cytochrome *c* oxidase, the so called electron backflow. Photodissociation of CO bound to the mixed valence enzyme lowers the apparent midpoint potential of heme a_3, causing a reverse flow of electrons (relative to the physiological pathway) from the binuclear center to heme *a* and to Cu_A (Boelens and Wever, 1979; Boelens *et al.*, 1982; Brzezinski and Malmström, 1987; Morgan *et al.*, 1989; Oliveberg and Malmström, 1991; Verkhovsky *et al.*, 1992; Georgiadis *et al.*, 1994). The Göteborg group in 1991 observed two processes with optical signals at 445 nm and 605 nm and apparent time constants of 3-5 µs and 77 µs, respectively, following the photolysis of the bovine heart cytochrome *c* oxidase mixed-valence CO complex (Oliveberg and Malmström, 1991). The two phases were proposed to be associated with the electron transfer between heme a_3 and heme *a* and between heme *a* and Cu_A, respectively. Verkhovsky *et al.*, (1992) confirmed this assignment by measuring the whole spectra of these phases in the Soret region. Electron transfer between the high- and low-spin hemes has also been observed on a microsecond time-scale upon photolysis of CO from wild-type cytochrome bo_3 and cytochrome oo_3 from *E. coli* (Morgan *et al.*, 1993; Brown *et al.*, 1994). In both cytochrome bo_3 and a mutated form of this enzyme which incorporates two heme O moieties hence cytochrome oo_3, the same electron transfer process was also apparently observed on faster and slower time-scales (Morgan *et al.*, 1993).

CO photolysis from the mixed-valence state of cytochrome *c* oxidase was studied in detail in the laboratory of Einarsdóttir. They used an optical multichannel spectrophotometric analyzer to monitor the intramolecular electron transfer in bovine heart cytochrome oxidase (Einarsdóttir *et al.*, 1992; Georgiadis *et al.*, 1994; Einarsdóttir *et al.*, 1995). This method allows collection of time-resolved spectra over a wide spectral range simultaneously on time-scales of tens-of-nanoseconds to seconds. The results from their analyses are in agreement with those of

Oliveberg and Malmström, (1991) and Verkhovsky *et al*., (1992), but indicate that in addition to the two electron transfer steps, a conformational change at heme a_3 may precede the electron transfer between the two hemes. According to their interpretation, as was already suggested by Brzezinski and Malmström, (1987), this conformational change may be a prerequisite for the subsequent heme-heme electron transfer.

The intramolecular electron transfer in cytochrome *c* oxidase has also been investigated using photoactivatable compounds as electron donors to the enzyme. In experiments in which a 1-methylnicotinamide radical generated by pulse radiolysis (Kobayashi *et al.*, 1989) or a photoactivatable tris(2,2'-bipyridyl)ruthenium (II) complex (Nilsson, 1992) were used as an electron source, Cu_A was found to be the primary electron acceptor. The apparent time constant of 50 μs for the electron transfer between Cu_A and heme *a* is similar to the value obtained following photodissociation of the mixed-valence CO complex. This demonstrates that the forward and backward rates of the electron transfer between heme *a* and Cu_A in cytochrome *c* oxidase are the same.

2.4 Proton pathways

During the catalytic cycle of dioxygen reduction to water in cytochrome *c* oxidase, protons in addition to electrons need to be brought to the binuclear site, which is buried deep in the membrane. Therefore, there is a requirement for specific pathways for proton transfer inside the hydrophobic part of the enzyme. Mutagenesis studies have been intensively used to elucidate and study the proposed proton pathways (channels).

Based on the results of site-directed mutagenesis studies (Hosler *et al.*, 1993; Thomas *et al.*, 1993; Garcia-Horsman *et al.*, 1995) and in agreement with the crystal structure of the *P. denitrificans* cytochrome aa_3 (Iwata *et al.*, 1995), at least two possible proton transfer pathways have been suggested. The shorter one, referred as K-pathway, leads to the binuclear center via the highly conserved residues Su I-Lys 354, Su I-Thr 351 and Su I-Tyr 280 located in transmembrane helices VI and VIII and the hydroxyl group of the heme a_3 hydroxyethylfarnesyl chain. The second (longer) D-pathway involves Su I-Asp 124 and a number of conserved polar residues (Su I-Asn 199, Su I-Asn 113, Su I-Asn 131, Su I-Tyr 35, Su I-Ser 134 and Su I-Ser 193).

Long-standing discussions of the function of the described proton channels continue at present. Mutations in the D- and K-channels block enzymatic activity at different stages of the catalytic cycle. Following the original observation of the abolition of proton pumping by mutations of the conserved aspartate residue in the D-channel (D135 in cytochrome bo_3 from *E. coli*; (Thomas *et al.*, 1993)), this structure has been speculated to be a "pumping channel" (Iwata *et al.*, 1995). Mutations in other residues within either the K-channel or the D-channel result in severe inhibition of steady-state turnover in both the *E. coli* bo_3 and *P. denitrificans* aa_3 oxidases (Thomas *et al.*, 1993; Fetter *et al.*, 1995; Garcia-Horsman *et al.*, 1995). According to Konstantinov *et al*., (1997), the D-channel is likely to be involved in the uptake of both the so called "chemical" protons (used for oxygen to water reduction) and "pumped" protons (used to create $\Delta\tilde{\mu}_{H^+}$) at least in the **F**→**O** transition. The K-channel is probably idle at this part of the reaction and is likely to be used for loading of the enzyme with protons at some earlier steps of the catalytic cycle. Later, the Helsinki Bioenergetics Group demonstrated that only the first proton during the reduction of the enzyme is taken up *via* K-channel and all other "chemical" and "pumped" protons are transferred through the D-channel (Wikström *et al*., 2000).

2.5 Oxygen and water channels

For the beef heart cytochrome *c* oxidase, three hydrophobic channels have been described and suggested as potential pathways by which oxygen could reach the binuclear site (Tsukihara *et al.*, 1996). For each of the three proposed channels dynamic side chain movements would still be required to allow oxygen diffusion. The postulated channels start at the protein-membrane interface near the center of the lipid bilayer where the oxygen solubility is much higher than in the aqueous phase. One of these channels has also been identified in *P. denitrificans* cytochrome aa_3 by mutagenesis studies (Riistama, 2000; Riistama *et al.*, 2000). It begins in the V-shaped cleft of subunit III directly above a tightly bound lipid molecule and leads through subunit I into the binuclear site.

The final product of the reaction catalyzed by heme-copper oxidases is water. At the maximal turnover rate of the bacterial cytochrome *c* oxidase, the enzyme produces 2000 water molecules per second. This is a considerable amount of water produced, therefore water exit pathways are probably necessary. A hydrophilic cleft between subunit I and II proceeds from the binuclear site to the surface of the protein. This channel involves a number of charged residues and the Mg binding site. Tsukihara *et al*. (1996) suggested that this structure serves as an exit pathway for the produced water. Iwata *et al*., (1995), who favors a direct coupling of proton pumping, described this cleft as the exit pathway of the pumped protons from the binuclear site to the outside.

2.6 Catalytic cycle

The typical turnover rate for bovine cytochrome *c* oxidase is in the order of 100 oxygen molecules per second and one turnover of the enzyme takes about ten milliseconds. The bacterial enzyme functions at a rate even faster than that. Each single turnover of the enzyme involves a number of chemical intermediates and the first intermediates of the reactions appear within a few microseconds.

The internal reactions of partially or fully reduced unliganded cytochrome *c* oxidase with dioxygen are so fast that studies by conventional stopped-flow techniques do not provide sufficient time resolution. The reaction of cytochrome *c* oxidase with oxygen is usually studied by the flow-flash technique developed by Gibson and Greenwood (Gibson and Greenwood, 1963; Greenwood and Gibson, 1967), which involves the photodissociation of CO from reduced heme a_3 in the presence of oxygen. Transient optical absorption studies have provided information about the kinetics of the internal electron transfer processes (Gibson and Greenwood, 1963; Greenwood and Gibson, 1967; Hill and Greenwood, 1984; Hill *et al.*, 1986; Orii, 1988; Oliveberg *et al.*, 1989; Blackmore *et al.*, 1991; Hill, 1991; Oliveberg and Malmström, 1992; Hill, 1994; Verkhovsky *et al.*, 1994) and more recently proton uptake (Oliveberg *et al.*, 1991; Hallén and Nilsson, 1992; Mitchell *et al.*, 1992; Hallén *et al.*, 1993; Hanson *et al.*, 1993; Hallén *et al.*, 1994; Mitchell and Rich, 1994). Low-temperature optical absorption and EPR trapping experiments (Chance *et al.*, 1975; Clore *et al.*, 1980; Karlsson *et al.*, 1981; Hansson *et al.*, 1982; Blair *et al.*, 1985; Morgan *et al.*, 2001) and time-resolved resonance Raman studies (Varotsis *et al.*, 1989; Han *et al.*, 1990; Ogura *et al.*, 1990; Varotsis and Babcock, 1990; Ogura *et al.*, 1993; Varotsis *et al.*, 1993) have yielded information about the transient intermediates generated during the dioxygen reduction reaction. Other probes of cytochrome *c* oxidase dynamics include time-resolved infrared (Dyer *et al.*, 1989; Dyer *et al.*, 1991; Stoutland *et al.*, 1991; Woodruff, 1993; Woodruff and Dyer, 1993; Dyer *et al.*, 1994) and time-resolved magnetic circular dichroism (Goldbeck *et al.*, 1991; Woodruff *et al.*, 1991; Goldbeck *et al.*, 1992) spectroscopies. Recently different kinds of electrometric methods were

used to study the oxygen reaction (Verkhovsky *et al.*, 1997) and partial steps during the reaction (Zaslavsky *et al.*, 1993; Siletsky *et al.*, 1999; Ruitenberg *et al.*, 2000; Verkhovsky *et al.*, 2001). Based on these studies various models of the redox-linked proton translocation have emerged (Mitchell, 1988; Chan and Li, 1990; Saraste, 1990; Babcock *et al.*, 1992; Rousseau *et al.*, 1993; Hill, 1994; Morgan *et al.*, 1994; Michel, 1998; Wikström, 2000).

By utilizing all these methods it is possible to separate and identify the chemical intermediates of the catalytic cycle of cytochrome *c* oxidase and to study the steps of the reaction separately. The elucidation of the steps ultimately connected to proton pumping is of the highest importance. As the work presented in this thesis is associated with the study of the transitions between intermediates and is focused on charge translocation across the lipid membrane, the view of the chemical cycle represented here is consistent with ideas previously known. The scheme of the catalytic cycle and the proton pumping steps of cytochrome *c* oxidase are shown in Fig. 2.

2.6.1 Intermediates

O. We start our examination of the catalytic cycle of cytochrome *c* oxidase from the fully oxidized state (**O**) where all four redox centers present in the enzyme are in their oxidized state. There are two different forms of the oxidized state, known as fast and slow, or pulsed and resting, respectively (Moody *et al.*, 1991). The Soret absorption maximum of the fast form of the oxidase is 424 nm, whereas that of the slow form of the oxidase is at 417 nm, with the "slow" oxidase showing characteristic EPR signals arising from the binuclear center, at g≈12 and

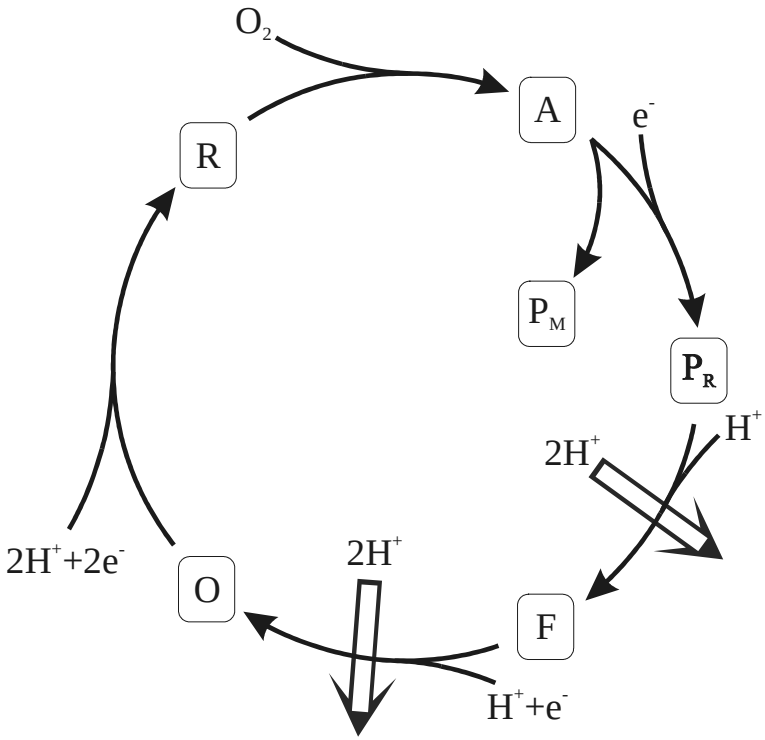

Figure 2. The chemical cycle of cytochrome *c* oxidase. Letters in the figure denotes the intermediate states of the binuclear site during the cycle.

g=2.95, that are not seen in the fast form of the enzyme (Beinert and Shaw, 1977; Greenaway *et al.*, 1977; Brudvig *et al.*, 1981; Cooper and Salerno, 1992). The binuclear center in the slow form of the oxidase is extremely un-reactive, both to inhibitory ligands such as cyanide (Brudvig *et al.*, 1981; Baker *et al.*, 1987) and to electron donors such as hydrogen peroxide (Baker *et al.*, 1987) and carbon monoxide (Morgan *et al.*, 1985). It is only slowly reduced by dithionite (Wrigglesworth *et al.*, 1988). However, reduction and re-oxidation of the binuclear center (pulsing) is sufficient to return the enzyme to the fast form (Antonini *et al.*, 1977; Brunori *et al.*, 1987). The difference between the pulsed and resting forms of the oxidized enzyme is still subject to dispute but most likely there is an internal ligand bound to the binuclear site after turnover is finished. This ligand, possibly a water molecule and the product of the reaction, most likely dissociates and diffuses away from the binuclear site with a time constant of the lifetime of the pulsed form. The other possibility is the opposite, that after oxidation of the enzyme some ligand binds in the binuclear site and slows down the reduction.

R. In cytochrome *c* oxidase in order for the reaction to begin, an oxygen molecule must bind to the binuclear center. Oxygen will only bind to the binuclear site if both metal centers are reduced. The enzyme is usually reduced using a strong reductant, for example dithionite or the combination of ascorbate and TMPD. In either case the enzyme is reduced fully, implying that the binuclear site, heme *a* and Cu_A are reduced. When the binuclear site is reduced, carbon monoxide can also bind to heme a_3. The state of the enzyme where heme *a* and Cu_A are oxidized and the binuclear site is reduced can also be formed using CO. The binding of CO to heme a_3 lowers its midpoint potential and traps both centers in the binuclear site in their reduced form. This state of the enzyme, when CO is bound to the reduced binuclear site while the other redox centers remain oxidized, is called the mixed-valence state. This state is widely used for studies of intermediates in the cytochrome *c* oxidase reaction cycle.

It is energetically unfavorable to bring two electrons (negative charge) into the middle of the membrane without charge compensation. In order to comply with the principles of electroneutrality, protons (positive charge) should also be taken up. Measurements by the Gëteborg group of pH changes upon oxidation of the fully reduced cytochrome oxidase showed approximately 2.6 protons released per oxidase at pH 7-8 (Hallén and Nilsson, 1992). Mitchell and Rich (1994) report a similar number in the pH range 7.2-8.5. Their measurements indicate that 2.4 protons are preloaded into the enzyme during the full reduction. Of these protons approximately 2 are associated with the binuclear center and the remaining fractional proton with heme *a*/Cu_A (Mitchell and Rich, 1994).

A. During the reaction, an oxygen molecule binds to the binuclear site and forms the so-called compound **A**. Although the fully reduced enzyme contains four redox equivalents, the reaction with oxygen can be started with two to four electrons in the enzyme but two electrons in the binuclear site is the minimum number. The finding that carbon monoxide transiently binds to the reduced Cu_B on its path to heme a_3 (Woodruff *et al.*, 1991; Einarsdóttir *et al.*, 1993) suggests that oxygen also may follow the same route. However, the low occupancy of this intermediate has precluded its observation in the optical spectra.

The presence of the heme a_3-O_2 complex was observed and assigned for the first time by Chance *et al*., (1975) using the low-temperature (liquid nitrogen) triple trapping technique. Later, the existence of compound **A** was confirmed at room temperature by Hill and Greenwood, (1983) and Orii, (1988) when the reaction was started from the mixed-valence state. However these authors subsequently disproved the room temperature existence of compound **A** when the reaction was started from the fully reduced state. Verkhovsky *et al*., (1994) proved the opposite and demonstrated that compound **A** does form in the course of the reaction starting from the fully reduced enzyme by showing the spectrum of this kinetic component. The time constant of the oxygen binding was found to be 8 μs at 1 mM of oxygen (maximum oxygen concentration in the water). The structure of compound **A** was also clearly established by resonance Raman

spectroscopy (see (Babcock and Wikström, 1992; Ferguson-Miller and Babcock, 1996) and references therein).

It is essential that the terminal oxidases have a high affinity for oxygen because the concentration of dissolved oxygen in the tissue is very low. However, the binding of oxygen to the respiratory heme-copper oxidases is very weak (Chance *et al.*, 1975; Verkhovsky *et al.*, 1994). On the other hand, cytochrome *c* oxidase reduces oxygen with a high rate. This paradox has been attributed to kinetic trapping during the rapid chemical reactions of oxygen inside the binuclear center (Chance *et al.*, 1975) and by the fast electron transfer between hemes (Verkhovsky *et al.*, 1994; Verkhovsky *et al.*, 1996). Instead of acquiring the oxygen molecule by tight binding, an energetically expensive alternative, the enzyme makes a rapid but loose attachment from which the oxygen molecule is subsequently "trapped" by the first redox step of the reaction. This achieves an apparent dioxygen affinity for the reduced binuclear center which is orders of magnitude more favorable than the oxygen binding affinity (Chance *et al.*, 1975; Verkhovsky *et al.*, 1994).

P. The next intermediate during the oxygen reaction is the so-called **P** intermediate. It was observed for the first time in low temperature experiments performed by Chance *et al.*, (1975) and at the time it was named compound **C**. Later Wikström (1981) observed this intermediate in the reverse reaction. The observed intermediate was two electrons more oxidized than the oxidized (**O**) enzyme. The author proposed that the chemical structure in the binuclear site was of the peroxy form of oxygen where the oxygen-oxygen bond is not broken, and therefore named it **P**. This intermediate can be observed starting either from the mixed-valence or the fully reduced enzyme. If the reaction of cytochrome *c* oxidase with oxygen is started from the mixed-valence state the **P** intermediate is observed with a time constant of 150 μs and is called $\mathbf{P_M}$. If the reaction is started from the fully reduced enzyme an intermediate $\mathbf{P_R}$ is formed within 30 μs (bovine enzyme). Since **P** is observable during the two-electron reaction (mixed-valence form) it was consistent with the peroxy chemical structure. The apparent difference between the two intermediates is that $\mathbf{P_M}$ is formed "using electrons from" the binuclear site only (two electrons) and for the formation of $\mathbf{P_R}$ the second electron is taken from heme *a*. Regardless of the fact that $\mathbf{P_R}$ and $\mathbf{P_M}$ are formed differently, both have the same absorbance spectrum with a distinctive absorbance peak at 607 nm in the alpha band (Morgan *et al.*, 1996).

The chemical structure of the **P** intermediate and particularly whether or not the oxygen-oxygen bond is broken in **P** is the subject of an on-going discussion in the oxidase field. It was proposed that at this stage of the enzymatic cycle the O-O bond of oxygen is still intact, giving a species with the form $a_3^{3+} - O = O^{=}$ (Wikström, 1981). Weng and Backer (1991), however, interpreted their optical data to indicate that O=O bond cleavage had already occurred at **P** and that this species had a $a_3^{4+} = O$ structure at the binuclear center. The kinetic resonance Raman data showed that during the time span of $\mathbf{P_M}$ formation the signal of the $a_3^{4+} = O$ species has its maximum amplitude, when starting from the mixed-valence form of the oxidase (Proshlyakov *et al.*, 1996; Proshlyakov *et al.*, 1998). In addition, it was recently demonstrated using mass spectrometry that indeed the oxygen-oxygen bond is already broken in the $\mathbf{P_M}$ state (Fabian *et al.*, 1999). After the reaction of the mixed-valence enzyme with $^{18}O_2$, $H_2{}^{18}O$ is observed in the medium in the proportion 1:1 with the amount of enzyme. The reaction can not proceed further than $\mathbf{P_M}$ when started from the mixed-valence state therefore this finding demonstrates that the oxygen bond is already broken in the $\mathbf{P_M}$ state.

The transformation of bound oxygen in the oxy species to hydroxide (or water) and ferryl-oxo in **P** requires a total of four electrons. In the mixed-valence state apparently only three electrons are available in the binuclear center – two from heme a_3 as it is oxidized the +2 to +4 valence state and one from Cu_B as it is oxidized from cuprous to cupric. The source of the fourth electron is still unclear. There are several candidates, such as a porphyrin π-radical,

Fe(V), Cu(III), or a protein side chain radical (Morgan *et al.*, 1996; Proshlyakov *et al.*, 2000). Yoshikawa *et al*. (1998) provided striking crystallographic evidence that strongly supports the latter possibility. They showed that Su I-Tyr 280 in the binuclear site is cross-linked to one of the Cu_B ligands, Su I-His 276 with the phenol head group oriented so that the –OH group points directly into the oxygen binding cavity. The Frankfurt group has reported similar crystallographic data for the bacterial enzyme (Ostermeier *et al.*, 1997) and Buse *et al*., (1999) have recently reported biochemical data that support the occurrence of the His-Tyr crosslink. Recent EPR data indicates the presence of tyrosyl radicals when peroxide is added to the resting enzyme, although the specific side chains involved have not been identified (Chen *et al.*, 1999; MacMillan *et al.*, 1999). There is another indication that the Su I-Tyr 280 is involved in the oxygen reaction (Proshlyakov *et al.*, 2000). These authors used a radioactive iodide labeling of peptide to probe radical formation in the cross-linked Su I-His 240 – Su I-Tyr 244. They specifically trapped the Su I-Tyr 280 radical and showed that it is indeed formed in $\mathbf{P_M}$. Unfortunately, the efficiency of the labeling of the formed radical was very low. Taken together these results suggest that the cross-linked tyrosine could be the source of the fourth electron in the activation and reduction of oxygen by cytochrome *c* oxidase. When the reaction is started from the fully reduced state, the fourth electron is available from heme *a* and is transferred to the binuclear site during **P** formation. There is no evidence or need for the formation of any kind of radical in the reaction of fully reduced enzyme with oxygen.

The main difference between the course of the reaction from the fully-reduced and mixed-valence states is the fact that heme *a* is initially reduced in the fully-reduced enzyme. Optical experiments have indicated that a large fraction of heme *a* becomes oxidized at the same time as **A** decays (Hill, 1991; Hill, 1994), and this was supported by the resonance Raman studies (Han *et al.*, 1990), who concluded that the decay of compound **A** is accompanied by transfer of the electron from heme *a* to the binuclear center. Thus, the ready availability of an electron in heme *a* appears to be the source of the difference between the fully reduced and mixed-valence reactions. Optical spectroscopy at low temperatures (Morgan *et al.*, 1995) indicated that the $\mathbf{P_R}$ intermediate was similar to the $\mathbf{P_M}$ intermediate, but clearly different from the subsequent ferryl state **F** that has an absorption maximum near 580 nm; this has since been confirmed at room temperature (Sucheta *et al.*, 1998). The chemical structure of the $\mathbf{P_R}$ state is much more obscure than that of $\mathbf{P_M}$. Unfortunately, the existence of neither the peroxy nor ferryl structures in the binuclear center has been confirmed by resonance Raman data at this state. Recently a breakthrough in understanding the structure of $\mathbf{P_R}$ was made using the EPR technique. Morgan *et al.*, (2001) used the triple trapping method to measure simultaneously the EPR and optical absorbance kinetics during the reaction of fully reduced cytochrome *c* oxidase with oxygen. In the time span of $\mathbf{P_R}$ formation, which was simultaneously monitored optically, they studied the unusual EPR signal observed earlier by the Göteborg group (Hansson *et al.*, 1982). This particular EPR signal consists of four bands between g=2 and g=2.5 which are extremely difficult to saturate. The optical spectrum of $\mathbf{P_R}$ and its unusual EPR spectrum suggests that the oxygen-oxygen bond is broken in $\mathbf{P_R}$ and the structure of the binuclear center is Fe(IV)=O Cu(II), probably with OH^- as a ligand on the copper ion (Morgan *et al.*, 2001). In this case, the only difference between $\mathbf{P_R}$ and $\mathbf{P_M}$ is the formed tyrosyl radical in $\mathbf{P_M}$, which most likely never forms if the reaction is started from the fully reduced enzyme.

F. In contrast to $\mathbf{P_M}$, the $\mathbf{P_R}$ intermediate is unstable and rapidly decays into the **F** state with no further electron transfer into the binuclear site. The time constant of this transition is 80 μs for bovine and 60 μs for the *P. denitrificans* enzyme. The optical spectrum of **F** in the alpha region drastically changes; the absorbance peak appears now at 580 nm and it is much broader and is less intense compared to the spectrum of **P** (Wikström, 1981). The ferryl intermediate was originally observed in reversed electron-transfer experiments (Wikström, 1981), where it was shown to result from one-electron oxidation of the ferric/cupric state of the

binuclear center, an assignment supported by low-temperature trapping (Blair *et al.*, 1985). This intermediate was observed in optical flow-flash measurements at room temperature (Orii, 1988) and the $a_3^{4+}=O$ structure has been confirmed by time-resolved Raman experiments (Han *et al.*, 1990; Ogura *et al.*, 1990; Varotsis and Babcock, 1990).

According to the latest view (Morgan *et al.*, 2001), both the $\mathbf{P_R}$ and **F** intermediates have the same structure of the oxygen adduct ($a_3^{4+}=O$). The main difference is that the Cu_B ligand in **F** is not OH^- as in $\mathbf{P_R}$, but HOH with one of the hydrogen atoms from the water molecule forming a strong hydrogen bond to the oxygen adduct on heme a_3. This interaction explains the absence of the unusual EPR signal in **F**, which is caused by increased electronic coupling between the metal centers in the binuclear site. The absorbance spectra of these intermediates also differ in the alpha region and this may also be caused by this strong hydrogen bond.

The last electron, which at the **F** state is equilibrated between heme *a* and Cu_A, enters the binuclear site and reduces the oxygen completely (**O** state). The **F** to **O** transition happens in two phases with time constants of 500 μs and 2.5 ms. The binuclear site in the **O** state is Fe(III) Cu(II) with HOH bound to heme a_3 and OH bound to Cu_B (Morgan *et al.*, 2001).

2.7 Proton pumping

The mechanism of the redox-linked proton pump has remained elusive since the discovery of the proton translocation function of cytochrome oxidase by Mårten Wikström in 1977 (Wikström, 1977). These studies which were carried out with rat liver mitochondria, and subsequent studies on reconstituted bovine heart enzyme in phospholipid vesicles (Wikström and Saari, 1977; Krab and Wikström, 1978; Casey *et al.*, 1979), showed that for each oxygen molecule reduced, cytochrome *c* oxidase translocates four protons from the inside to the outside of the membrane using the free energy of the oxygen reduction reaction as the driving force.

The reaction proceeds from the reduced enzyme (**R**) through "peroxy" (**P**) and ferryl (**F**) intermediates to the fully oxidized enzyme (**O**). Not all the steps in the reaction are energetically equal. Insight into which steps of the reaction are associated with the large drop of potential energy would answer a lot of questions about the mechanism of proton pumping in cytochrome *c* oxidase. Wikström showed that by placing a backwards driving force on the enzyme in mitochondria ($\Delta\psi$ and high E_h), the oxygen reaction could be partially reversed from the **O** state, leading first to **F** and then to **P** (Wikström, 1981). Thermodynamic analysis of this reaction (Wikström and Morgan, 1992) led to the conclusion that all the work required for proton pumping is done in the two electron transfer steps: **P**→**F** and **F**→**O**, consistent with translocation of two protons at each step (Wikström, 1989). These transitions are associated with the largest drop of energy. As calculated by Wikström and Morgan (1992), the drop of energy is 1.1 V and 1.2 V during **P**→**F** and **F**→**O** transitions, respectively. All other transitions in the oxygen reaction are not associated with a significant release of energy. For example, on the basis of quantum chemical calculations Blomberg *et al.*, (2000) concluded that the formation of $\mathbf{P_M}$ from compound **A** is nearly isergonic.

Using the temporal comparison of optical and electrometrical data Verkhovsky *et al.*, (1997) demonstrated that the **P**→**F** and **F**→**O** transitions are associated with an equal amount of transferred charge. Unfortunately, it is difficult to calibrate the electrometric response and at the time it was impossible to say how many charges were transferred during each transition.

Konstantinov's group used an electrometric measurement system to study the **F**→**O** transition specifically (Zaslavsky *et al.*, 1993; Konstantinov *et al.*, 1997). The **F** form of the enzyme was prepared by addition of hydrogen peroxide and ruthenium bipyridyl ($Ru(bipy)_3$) was used to photoinject an electron into the enzyme. The electron travels via Cu_A to heme *a* and

hence to the oxygen-reduction site where it reduces **F** to **O**. Two electrogenic phases were observed, corresponding to fast electron transfer from Cu_A to heme *a* followed by slower reduction of **F** to **O**. The amplitude of $\Delta\psi$ generated in the **F**→**O** transition was found to be 4 times the amplitude of the fast phase. The main conclusion in this work was that the **F**→**O** transition is associated with the pumping of two protons. Later Siletsky *et al*., (1999), using the same electrometric technique, demonstrated the same number for the **P**→**F** transition. Unfortunately, the number of translocated protons determined from these experiments crucially depends on the dielectric depth of the hemes in the membrane (**d**). In this work the value 0.5 was used (Hinkle and Mitchell, 1970). This important parameter was first evaluated by Hinkle and Mitchell using the electrochemical titration. This value is on the high side, especially taking into account the crystallographic data which shows that geometrical depth of the hemes in the membrane is about 0.3. The large amount of water molecules in the upper part of subunit I suggests that the parameter **d** could be even smaller than 0.3.

3. Aims of the present study

The catalytic function of cytochrome *c* oxidase is ultimately coupled to proton pumping and to creation of $\Delta\psi$ across the phospholipid membrane of the cell. The electrometric study of the electrogenic reactions in cytochrome *c* oxidase, during the full and partial steps of the catalytic cycle, is the main task of this study. To be more specific, the main aims were:

1. To study the electrogenic reactions during the oxidative part of the catalytic cycle of cytochrome *c* oxidase from the bovine heart using a "flow-flash" setup of the electrometric method and to find the steps in the reaction which are coupled to charge movements.

2. To study the electrogenic reactions in the cytochrome *bd* oxidase from *E.coli*. As this enzyme reduces oxygen but does not pump protons it is interesting to compare the electrogenic steps with those of the bovine enzyme.

3. To study the electrogenic response of bovine cytochrome *c* oxidase during the complete catalytic cycle – oxidative and reductive parts – and to compare the electrogenicities in these phases.

4. To use the electrometric method to study the backflow reactions after CO photolysis in the partially reduced enzyme. To calibrate the electrometric responses during the oxidative part of the reaction with oxygen using this method in combination with optical absorption spectroscopy,.

5. To study and compare the electrogenicities between cytochrome aa_3 from *P. denitrificans* and cytochrome *c* oxidase from bovine heart. To use mutant forms of the bacterial enzyme to study which parts of the catalytic cycle are altered in each mutant.

4. Materials and Methods

Electrometric measurement procedure. The direct, time-resolved, electrical measurement is based on a method developed by Drachev and co-workers (Drachev *et al.*, 1974; Drachev *et al.*, 1978). In the present system $Ag/AgCl_2$ electrodes record the voltage between the two compartments of a cell, separated by a measuring membrane, consisting of a lipid-impregnated teflon mesh (Fig. 3). Vesicles, into which the enzyme has been reconstituted, are forced to associate with this measuring membrane. The voltage across the measuring membrane follows the $\Delta\psi$ across the vesicle membranes proportionally, allowing the kinetics of charge translocation to be recorded. Typically the measuring membrane has a resistance of about 5 GΩ and the measured $\Delta\psi$ decays with a time constant of about 5 seconds.

Preparation of samples: Proteoliposomes were added to one of the two compartments of the cell and were forced to associate with the measuring membrane by addition of 10-15 mM $CaCl_2$ (the same amount of $CaCl_2$ was added to both compartments) followed by an incubation of between 2 and 3 hours. Incubation was carried out at pH 7 (usually in 100 mM BTP). The cell was enclosed in gas-tight box, which had been purged with argon, and anaerobicity was reached by addition of 50 mM glucose, 50 µg/ml catalase and 130 µg/ml glucose oxidase. After incubation, the cell was removed from the box and the liquid in both compartments was exchanged for argon saturated buffer (usually 100 mM HEPES, pH 8). Immediately thereafter, 50 mM glucose, 50 µg/ml catalase and 130 µg/ml glucose oxidase were added to keep the sample anaerobic. 100 µM TMPD, 100 µM DCPIP, 10 µM hexaammine ruthenium and 0.5 µM cytochrome *c* were added as redox mediators, and 60 mM ferrocyanide was used as a redox buffer. After the additions, the $Ag/AgCl_2$ electrodes (World Precision Instruments, Stevenage, Hertfordshire, UK), which had been kept in an anaerobic environment, were inserted, the cell was returned to the gas-tight box which was , purged with argon and then CO (100%). A computer-driven syringe pump (SP200i, World Precision Instruments) was used to inject 50 µl of oxygen-saturated buffer (rate 5 ml/min) via a 2.5 ml gas-tight syringe and a long 22S RN needle (Hamilton, Reno, Nevada). The jet from the needle was directed at the measuring membrane (a 4 mm circle), producing a local high concentration of oxygen for the time of the reaction. The reaction was started by a laser flash (Quantel Brilliant frequency doubled YAG, pulse energy: 180 mJ) 200 ms after the end of the injection. The oxygen concentration at the

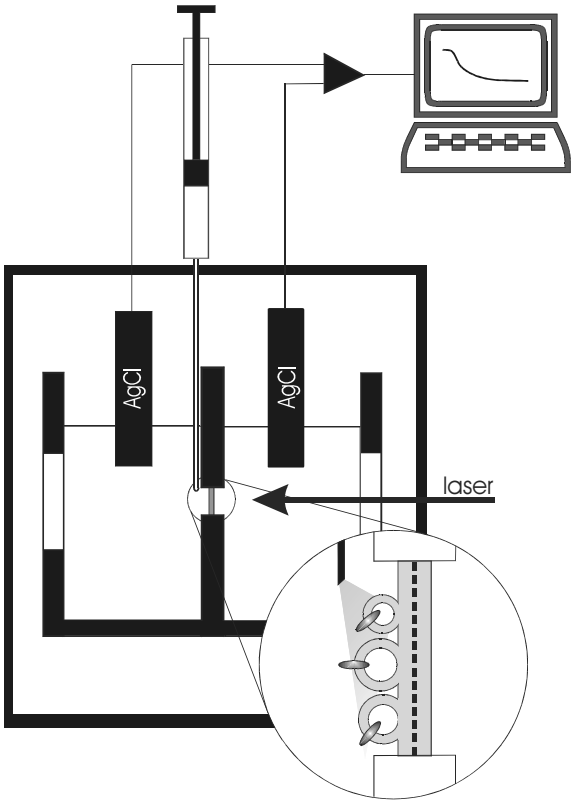

Figure 3. The scheme of the electrometric setup.

membrane after injection is almost certainly close to the saturation value of 1.2 mM, because increasing the injected volume does not decrease the lag or increase the rate of the "fast" phase (see below) and the rates obtained by fitting are consistent with those from optical data obtained at close to saturating oxygen concentrations. For experiments in which the redox potential (E_h) of the medium was titrated, the E_h was initially raised by the addition of a small volume of concentrated anaerobic ferricyanide. After that, the glucose-glucose oxidase system itself slowly lowered the E_h, and kinetic measurements could be initiated when the appropriate E_h values were reached. The E_h of the system was determined from the voltage between a platinum wire (measuring electrode) and the ground $Ag/AgCl_2$ electrode (reference electrode, +200 mV) .

Enzyme preparation. Bovine heart cytochrome *c* oxidase was prepared by a modification of the method of Hartzell and Beinert (1974). During enzyme preparation, the pH was kept above 7.8 and Triton X-114 and cholate were added on the basis of cytochrome aa_3 concentration rather than total protein (Baker *et al.*, 1987). No ethanol was used to remove the Triton X-114 after the red/green cut; instead, the green pellet was repeatedly resuspended in the preparation buffer and centrifuged, until the amount of detergent was significantly reduced, as judged by the extent of bubbling when the supernatant was shaken (usually three or four exchanges).

Reconstitution of the enzyme into phospholipid vesicles To remove cytochrome *c* oxidase dimers and other possible contaminants from the preparation, the enzyme was purified on a sucrose gradient as described by Finel and Wikström (1986). Reconstitution of the enzyme into proteoliposomes was carried out as follows: 150 µl of cytochrome *c* oxidase from the sucrose gradient (concentration approximately 4-8 µM) was diluted to a volume of 1 ml with a suspension of sonicated, pre-formed liposomes containing 80 mg/ml lipid, 2% (w/v) cholic acid and 100 mM potassium-HEPES (pH 7.4), and was mixed for 20 min at room temperature. Removal of detergent was performed according to Rigaud *et al.* (1995) using Bio-Beads SM-2 absorbent (Bio-Rad). The scheme for detergent removal is shown in table 1 (**I**). It should be noted that, in order to slow down the removal of detergent, the first few additions of Bio-Beads were performed at 4°C. This increased the yield of reconstituted enzyme. At the end of the procedure, vesicles with a respiratory control ratio of 15-20 were typically obtained. Proteoliposomes were frozen and stored in liquid nitrogen. The final concentration of enzyme in the vesicles, determined spectroscopically using $\varepsilon_{604\text{-}620}$(reduced-oxidized)=0.024 $cm^{-1}\cdot\mu M^{-1}$, was typically 0.3-0.5 µM.

Measurement electronics. The measurement system consisted of a home-made preamplifier whose output could be recorded using two different types of PC-based digitizers: an 8-bit PCIP-SCOPE (Metrabyte) running DA90 acquisition software (Alexander Drachev, Tempe, AZ) and a 12-bit CompuScope 512 (Gage Applied Sciences, Montreal, Canada) running GageScope data acquisition software. Timing was controlled by a CTM-05 counter-timer board (Metrabyte).

Sequential reaction model. In order to fit the electrometric oxygen reaction data, a model of a sequential first order chemical reaction with five steps was used. Each step in such a reaction is characterized by a first-order rate constant k_i (i=1,…,5). The overall reaction can be characterized mathematically by a set of six differential equations where the six solutions represent the concentration of the six intermediates at any time. However, unlike a spectroscopic measurement, which tracks the formation and decay of the various reaction intermediates, the electrometric measurement tracks transport of charge across the membrane. The solutions of the differential equations each reflect the lifetime—formation and decay—of a given intermediate (the first solution shows only decay of the starting material and the last shows only the formation of the final product). These solutions cannot be used directly as a basis set to fit electrometric data because, the quantity measured is net movement of charge, which does not necessarily move back in the next step; that is, there is no process corresponding to obligatory decay of one

intermediate as the next intermediate is formed. Thus, instead of using the solutions of the differential equations directly as the basis set for the fit, we constructed a cumulative sum of these solutions (1, 1+2, 1+2+3, ...) so that each vector in the basis set corresponds to the transition which takes place in one kinetic phase—in this case, the movement of one charge (q) through an arbitrary unit distance in the direction of the membrane normal. The rate constants and amplitudes were then varied to obtain the best fit to the experimental data using the *constr* constrained fitting function of MATLAB (Mathworks, South Natick, MA).

5. Results and discussion

5.1 Characterization of the electrometric response during the reaction with oxygen.

5.1.1 The reaction of bovine cytochrome c oxidase with oxygen

The time-resolved electrometric method allows direct measurement of the electrical potential ($\Delta\psi$) generation across the phospholipid bilayer with sub-microsecond time resolution. This makes it possible to observe the development of $\Delta\psi$ within a single turnover of cytochrome *c* oxidase. We have used this methodology to study the reaction of the reduced cytochrome *c* oxidase with oxygen, using a modification of the "flow-flash" experiment. In this case, in order to obtain the required time resolution, oxygen is added to the CO-inhibited enzyme in the dark, and the reaction initiated rapidly by photolyzing the CO (Gibson and Greenwood, 1963). After photolysis CO instantly leaves heme a_3 allowing oxygen to bind to the binuclear center and for the reaction to start. Using such an approach it is possible to monitor the reaction in a coherent way in a 100% population of the enzyme.

A typical electrometric recording of the reaction of the fully reduced cytochrome *c* oxidase with oxygen is shown in the main panel of **I**, Fig. 2. The bottom panel shows the difference between the experimental data and a theoretical fit based on a sequential reaction model. The early part of the reaction is taken up by an initial lag (**I**, Fig. 2, inset), after which $\Delta\psi$ develops in three phases. The lag is too long to be caused by a single reaction step. In the fit shown, the lag has been modeled as two sequential reaction steps, the first with a time constant of 10 μs and the second 25 μs. Spectroscopic measurements on the same reaction have found two processes with rate constants very similar to these, which were assigned as the initial binding of oxygen to heme a_3 to form the ferrous-oxy intermediate (**A**) followed by the transition from **A** to a formal peroxy intermediate (**P**). In our fit, the amplitude of the first reaction in the lag was defined as zero. The amplitude of the second sequential step in the reaction was allowed to float in the fitting process, but even so, the fit found it to have a very small, positive, value, 3.1 ±1.5 percent (n=14) of the total amplitude, whereas all other phases are negative in sign. This confirms that very little, if any, net charge movement occurs during this part of the reaction.

After the lag $\Delta\psi$ begins to grow. The fastest component of this increase has a time constant of about 80 μs and contributes 52.6 ±5.3 percent of the total amplitude of the response. The rate of this phase is similar to the rate of the process spectroscopically assigned to the transition of **P** to the ferryl intermediate **F** (**P**→**F** transition).

This is followed by two slower phases with time constants of 0.5-1 ms and 1-5 ms respectively, which together make up the remaining amplitude (50.5 ±4.1 percent of the total; the sum of fast and slow phase amplitudes is slightly larger than 100 percent because of the small positive contribution of the second lag phase). Two phases with approximately the same rates as these are seen in optical studies of the reaction of fully reduced cytochrome *c* oxidase with oxygen. Based on their visible spectra both phases reflect conversion of **F** to the oxidized form of the enzyme **O** (**F**→**O** transition; M. I. Verkhovsky and J. E. Morgan unpublished data; see also Nilsson, (1992), Zaslavsky *et al*., (1993)).

When the four-electron reduced enzyme reacts with oxygen the reaction passes through intermediates **P** and **F** to ultimately produce the oxidized enzyme **O**. It is possible to control how far along this sequence of intermediates the reaction proceeds by choosing the number of reducing equivalents initially in the enzyme (Chance *et al.*, 1975; Witt and Chan, 1987; Lauraeus *et al.*, 1993). If the enzyme initially contains three electrons the reaction only goes as far as **F**, whereas, if the enzyme contains two electrons the reaction is trapped at **P** state (**I**, Fig. 3).

We used this behavior to help assign the electrometrically observed phases, making measurements with the enzyme at various levels of reduction. In practice, this was done by varying the redox potential (E_h) of the medium with which the enzyme is in equilibrium prior to the start of the reaction. In the presence of CO, the two-electron reduced state is stable at relatively high redox potentials. Lowering the potential leads to populations of three- and then four-electron reduced enzyme (**I**, left hand side of Fig. 3). Thus, by making measurements beginning with the enzyme poised at different redox potentials, we were able to separate the electrometrically observed phases.

I, Fig. 3 (right hand side) shows examples of the time course of $\Delta\psi$ development when cytochrome *c* oxidase, poised at three different initial redox potentials, reacts with oxygen. At high redox potential (about 350 mV vs. NHE and higher) the CO-bound enzyme contains only two electrons, both of which are held in the binuclear center by CO, while the other two centers (Cu_A and heme *a*) remain oxidized (**I**, state I in Fig. 3 and scheme 1). When this two-electron reduced enzyme reacts with oxygen, the reaction proceeds only as far as the **P** intermediate. To a first approximation, **I**, Fig. 3 ($2e^-$ enzyme trace) shows, that no net charge movement takes place in this part of the reaction.

At a slightly lower redox potential, some of the enzyme will contain a third electron on either Cu_A or heme *a* (**I**, Fig. 3, states II and III). Electrometric recordings of the oxygen reaction starting at redox potentials close to 320 mV (**I**, Fig. 3, $3e^-$ enzyme trace) show the appearance of the "fast" phase (defined above), which was not present in the reaction of the two-electron reduced enzyme, clearly demonstrating that this fast phase is associated with the **P** to **F** transition. As the redox potential is lowered further, a population of the four-electron reduced enzyme appears. The amplitude of the fast phase increases and the "slow" phase appears, reflecting the fact that in the four-electron reduced population of enzyme, the reduction of oxygen can proceed to completion, with formation of the fully oxidized enzyme (**O**). Further lowering of the redox potential increases the four-electron enzyme population further increasing the amplitudes of both fast and slow phases (**I**, Fig. 3, $4e^-$ enzyme trace).

In this system the two- and four-electron reduced states of the enzyme can be obtained in essentially 100% yield as a starting point for the reaction, but the three-electron reduced enzyme exists in equilibrium mixture with two- and four-electron reduced species (**I**, scheme in Fig. 3). Thus, to further confirm the three-electron result, a control experiment was done with cytochrome bo_3 oxidase from *E. coli*, which had been prepared in such a way that bound quinol was removed (Puustinen *et al.*, 1996). As this preparation contains neither Cu_A nor bound quinol, the fully reduced enzyme contains only three reducing equivalents. When this enzyme reacts with oxygen, the development of $\Delta\psi$ (data not shown) takes place with essentially the same time course as in the bovine cytochrome *c* oxidase poised at the three-electron level (**I**, Fig. 3, $3e^-$ enzyme trace), confirming the assignment of the fast electrometric phase to the **P** to **F** transition.

5.1.2 The reaction of cytochrome bd with oxygen

Some bacterial species contain enzymes which are designed to function at low oxygen concentrations in order to keep the bacteria alive in extreme conditions. In *E. coli*, for example, such an enzyme is cytochrome *bd*. As with all other oxidases it catalyses the reduction of oxygen to two water molecules. On the other hand it was demonstrated that this enzyme does not pump protons across the membrane (Puustinen *et al.*, 1991) and it conserves the energy released during the reaction only by means of vectorial chemistry. Since this enzyme is not a proton pump (Puustinen *et al.*, 1991) but creates $\Delta\psi$ during catalysis (Miller and Gennis, 1985), it was interesting to study the reaction with oxygen using the electrometric method.

A typical electrometric recording during the reaction of the fully reduced cytochrome *bd* with oxygen is shown in **II**, Fig. 2. After the flash there is a small but reproducible lag phase (inset) after which the electrogenic response rises in a single exponential phase with a time constant of 60 μs. The kinetics of the response can be modeled reasonably well by a sequential reaction model A→B→C where A→B is electrically silent.

These two reaction steps match neatly with the two phases found in the spectrophotometric experiments by Hill *et al*., (1994). The appearance of the first phase in the electrometric data (A→B) as a lag is consistent with its assignment as an oxygen binding process. This is reminiscent of what has been seen in the cytochrome *c* oxidase and was discussed above, where the binding of oxygen is not electrogenic. The major electrogenic phase (B→C; 60 μs) corresponds well with the second phase reported by Hill *et al*., (1994) (80 μs). The ~1.3-fold difference between these values is probably not significant, even though the conditions of the experiments were slightly different in temperature (24-25 vs. 20ºC) and enzyme environment (lipids vs. detergent), the difference in the rates appears to be within the uncertainty of the spectrophotometric measurements (see Figures 3 and 4 of Hill *et al*., (1994)). There is a significant H_2O to D_2O solvent isotope effect on the major electrogenic phase with the fitted time constant increasing from 60 μs to 230 μs. There is no discernable effect on the lag.

It is instructive to compare the kinetics of $\Delta\psi$ generation by cytochrome *bd* and bovine cytochrome c oxidase (**II**, Fig. 3). The major, 60 μs, electrogenic phase in the cytochrome *bd* oxygen reaction can be seen to have a closely matching counterpart in the electrogenesis revealed by cytochrome aa_3 identified earlier as the **P→F** transition. There are however two clear distinctions between the enzymes.

First, in the reaction of cytochrome *c* oxidase with O_2, the development of $\Delta\psi$ includes an additional phase, which evolves on a millisecond time scale. This is explained by the fact that although fully reduced, cytochrome *bd* carries only three reducing equivalents, whereas cytochrome *c* oxidase carries four. The reaction of fully-reduced cytochrome *bd* with dioxygen stalls at the ferryl stage (**F**), but in cytochrome *c* oxidase the presence of a 4^{th} electron allows the reaction to continue one step past **F** to produce water, together with the fully-oxidized enzyme.

Second, in case of cytochrome *c* oxidase the lag phase is much more pronounced (**II**, Fig. 3, inset). In order to fit the $\Delta\psi$ generation data by cytochrome *c* oxidase, at least two sequential non-electrogenic, or very weakly electrogenic steps preceding the ~100 μs electrogenic phase must be included in the model. As discussed above, these steps correspond to binding of oxygen to the reduced enzyme (**R→A** transition) and conversion of the ferrous-oxy (**A**) intermediate to the "peroxy" intermediate (**A→P**). A similar lag is observed in the reaction of the bo_3-type quinol oxidase from *E. coli*, discussed above. In cytochrome *bd* the lag is much shorter and, as mentioned above, can be fitted by a single step in the kinetic model. This supports the conclusion from the spectrophotometric measurements ((Hill *et al.*, 1994) and below) that in cytochrome *bd* intermediate **A** decays directly to **F**. In contrast to the heme-copper oxidases, in the reaction of cytochrome *bd* with O_2 there is either no **P** intermediate or this intermediate is too short-lived to be detected.

In order to explore this reaction in more detail, we performed an optical control using a low temperature version of the "flow-flash" method (LTFF) in which the reaction is carried out at about –20ºC in order to slow it down to the point where the millisecond resolution of a diode array spectrophotometer can adequately capture the kinetics of the process (Morgan *et al*., 1996). This makes it possible to obtain a complete spectrum of the sample (500-700 nm) every millisecond as the reaction unfolds.

When fully reduced cytochrome *bd* reacts with dioxygen in the LTFF experiment, absorption changes begin immediately after the flash and reach completion within about 100 ms. Global analysis of the surface of spectra collected during the reaction reveal two clear transitions

(**II**, Fig. 1) in agreement with Hill *et al.*, (1994), Hill, (1994). At –20º C the two phases have time constants of ≤ 1 ms and 7.7 ms. The spectrum of the first phase has a peak at 650 nm and a trough at 630 nm, typical of π-donor ligand binding to reduced heme *d*, as expected for formation of the ferrous-oxy (**A**) intermediate (**II**, Fig. 1, dashed line). In addition, there may be some perturbation of the ferrous heme b_{595} spectrum as evidenced by minor absorption changes around 600 nm.

When cytochrome *bd* is prepared there is typically a population of the enzyme in which heme *d* is reduced with O_2 bound, i.e., a stable ferrous-oxy species (**A**). The bound O_2 can be removed by repeatedly exchanging the gas atmosphere of the sample with oxygen-free argon. In order to obtain a reference spectrum of compound **A** the spectral changes, which accompany removal of O_2, were measured. In the spectral region from 620 to 700 nm, this difference spectrum is almost exactly the inverse of the spectrum of the first phase of the O_2 reaction (**II**, Fig. 1). This supports the assignment of this kinetic phase as O_2 binding to reduced heme *d*. There are larger differences in the spectral region from 520 to 620 nm. This reflects electron redistribution in the argon-exchanged sample after O_2 is removed from heme *d*, a process analogous to "electron backflow" after photolysis of CO (below).

The ferrous-oxy intermediate (**A**) then decays in a monoexponential process to a state with increased absorption at 680 nm. There is simultaneous oxidation of heme b_{558} (the troughs at 560 and 530 nm are the α- and β-bands respectively). The 680 nm feature has been assigned to the ferryl-oxo (**F**) state of the enzyme on the basis of resonance Raman spectra (Kahlow *et al.*, 1991; Borisov *et al.*, 1995). It is thought that heme b_{595} also becomes oxidized in this phase, although it is possible that the small trough at 595 nm may be accounted for as part of the heme *d* ferryl-oxo spectrum. The reaction stops at this point—with O_2 reduced to the 3-electron level. The spectra of the two phases confirm the assignments of Hill *et al.*, (1994), however, the time constants are not comparable because of the ~40ºC temperature difference between the two sets of measurements.

In cytochrome *bd* the ferrous-oxy (**A**) intermediate appears to decay directly to the ferryl (**F**) state. In contrast, in cytochrome *c* oxidase (aa_3) an intermediate known as **P** ("peroxy") intervenes between these two states and is clearly resolvable under conditions similar to those of the present measurements (Morgan *et al.*, 1996). However, there are no indications of an analogous intermediate in the present data.

Another way to generate compound **P** in cytochrome *bd* is by reaction with hydrogen peroxide. H_2O_2 is known to react with heme-copper oxidases to produce **P** and/or **F** depending on the conditions (Wrigglesworth, 1984; Orii, 1988; Vygodina and Konstantinov, 1989; Weng and Baker, 1991; Fabian and Palmer, 1995). To investigate this possibility, the reaction of oxidized cytochrome *bd* with H_2O_2 was repeated under the same conditions where **P** had been identified in heme-copper oxidases (Morgan *et al.*, 1995). However, in contrast to the aa_3 and bo_3 oxidases, the peroxide reaction in cytochrome *bd* is monophasic. The difference spectrum for the single kinetic phase (**II**, Fig. 1, panel B) is identical to that of the final product formed upon addition of excess hydrogen peroxide to ferric cytochrome *bd* (Lorence and Gennis, 1989; Borisov *et al.*, 1995) which has been assigned to the oxo-ferryl species (**F**) (Kahlow *et al.*, 1991). There is thus no evidence for an intermediate corresponding to **P** of the heme-copper oxidases in the electrometric or spectrophotometric studies of the reaction of O_2 with reduced cytochrome *bd*, or in the reaction of H_2O_2 with the oxidized enzyme.

We have tried to trace and trap a **P** intermediate using three different optical techniques without success. This suggests that in cytochrome *bd* the **P** intermediate does not exist and compound **A** decays directly into the **F** intermediate. As this enzyme is designed to function at very low oxygen concentrations, the energy which might be used for proton pumping is used instead to stabilize compound **A**. This proves that the **P** intermediate is essential in the mechanism of proton pumping.

5.1.3 The electrometric flow-flash in the wild type form of the Paracoccus denitrificans cytochrome c oxidase.

Some bacteria contain a cytochrome *c* oxidase, which is very similar in structure and function to the bovine cytochrome *c* oxidase. One of those bacteria is *Paracoccus denitrificans*. The cytochrome *c* oxidase from *Paracoccus denitrificans* contains only four subunits, compared to 13 in the mammalian enzyme, but their structure is highly homologous to the bovine structure and the key residues of the proposed proton channels are at the same positions as in the mammalian enzyme. It contains the same redox centers, *i.e.* Cu_A and Cu_B, heme *a* and heme a_3 and the structure of binuclear center is the same. It is well established that the chemical cycle and the proton pumping stoichiometry of the bacterial enzyme are the same as that of the mitochondrial one. The main advantage of studying the bacterial aa_3 oxidase is that it is possible to make site-specific mutations of amino acids and then compare the mutant enzyme to the wild type. But first it is necessary to know the behavior of the electrometric response in the wild type enzyme.

The profile of the electrometric response when the fully reduced cytochrome *c* oxidase from *Paracoccus denitrificans* reacts with oxygen is the same as in the case of bovine aa_3 (unpublished data). It consists of three main electrogenic phases: the amplitude of the first phase makes about a half of the total response. The main difference between the responses of the two enzymes is that the rates of these kinetic phases are a little bit faster in the case of bacterial enzyme. The rate of the first electrogenic phase, which is coupled to the **P→F** transition is as fast as 60 μs compared to 80 μs in bovine case. The **F→O** transition consists of two phases; 300 μs and 2.5 ms. In the case of the mammalian enzyme these numbers are 1 ms and 5 ms respectively (unpublished data). The slightly higher rates of the intermediate steps in the reaction are consistent with the higher turnover rate of the aa_3 oxidase from *Paracoccus denitrificans*.

The similarity between electrometric signals of the cytochrome *c* oxidases from two different species imply the same mechanisms of oxygen chemistry and proton pumping in both enzymes. Even small differences in the structure or parameters, like the dielectric distance **d**, would show in the difference in the ratios of the phases in the electrometric signal.

5.1.4 Electrogenic steps during the oxygen reaction of the Paracoccus denitrificans R54M mutant

We have studied the mutant form of the *Paracoccus denitrificans* cytochrome *c* oxidase in which the arginine residue in position 54 of subunit I is changed to methionine. Already in 1983, in order to explain the unusual absorption spectrum of heme *a* in the bovine cytochrome *c* oxidase, Babcock and Callahan (1983) proposed that the formyl group of heme *a* forms a hydrogen bond to an amino acid side chain. Iwata *et al*., (1995) and Tsukihara *et al*., (1996) using the X-ray structure predicted that this amino acid should be arginine 54. Riistama *at al*., (2000) mutated this arginine and showed experimentally the influence of this amino acid on the spectrum of heme *a*. Changing Arg 54 to methionine breaks the hydrogen bond between this amino acid residue and the formyl group of heme *a*. This slight change of the heme-protein interaction alters the spectrum of heme *a*; the peak position of the alpha band appears at 590 nm, a shift to the blue side of the spectrum by 15 nm. This position of the peak in the alpha band would be an expected position for “normal” low spin heme *a*.

The other consequence of this mutation is the significant lowering of the redox midpoint potential of heme *a* (Kannt *et al*., 1999). This shift of the midpoint potential dramatically

changes the redox properties of the enzyme. In the wild type, if CO is present, both heme *a* and Cu_A reduce at approximately the same redox potential. In the case of R54M mutant, Cu_A will reduce first and heme *a* will reduce last. In addition, the gap between midpoint potentials is so large that it is possible to form 100% of the three-electron reduced enzyme. This is impossible in the case of wild type where there it is always a mixture of two-, three- and four-electron reduced enzyme populations.

The change in the midpoint potential of heme *a* also influenced the behavior of the mutant during the catalytic cycle of the enzyme. In this mutant, if the reaction was started at the fully reduced (four-electron reduced) state of the enzyme, the electrometric response showed the same rate of **P→F** transition as in the wild-type (**III**, Fig. 5). On the other hand, if the reaction was started at the three-electron reduced level, the behavior of the electrometric response was very different. For the three-electron reduced enzyme, after the initial lag (which is the same as in the wild-type enzyme) there was an electrogenic phase with a time constant of 13 ms. Using optical spectroscopy in **III** we demonstrated that this kinetic phase, according to an optical spectrum of the transition, corresponds to the **P→F** transition (**III**, Fig. 4). In this mutant enzyme the **P→F** transition is slowed down approximately 200 times when the reaction is started at three-electron reduction level.

As summarized in section 2.6.1 of this thesis, when the fully reduced, wild-type cytochrome *c* oxidase reacts with oxygen the peroxy intermediate is formed together with the oxidation of heme *a*. The peroxy intermediate formed in this way is called $\mathbf{P_R}$. On the other hand, if the same reaction was started from the two-electron reduced level, the peroxy intermediate is formed slower and an electron for O=O bond breakage is taken from the enzyme itself (for example the tyrosine residue). In this case the peroxy intermediate is called $\mathbf{P_M}$. The above discussed results can be explained as follows (**III**): If the oxygen reaction of the R54M mutant of *Paracoccus denitrificans* started from the fully reduced level (4 e^-) the reaction goes *via* the $\mathbf{P_R}$ intermediate. In this mutant the three-electron reduced enzyme differs from the wild type enzyme. Two electrons reside on the binuclear site as in the wild type. The third electron is not shared between heme *a* and Cu_A as in the wild type but is fully situated on Cu_A and there is a large barrier for this electron to enter the binuclear site *via* heme *a*. We propose that in this case in the reaction with oxygen the peroxy intermediate is formed using electrons from the binuclear site and $\mathbf{P_M}$ is formed instead.

According to the electrometric data for this reaction we observe the same amplitude for both $\mathbf{P_R}$→**F** and $\mathbf{P_M}$→**F** transitions. Since both responses were obtained using the same sample we can directly compare the amplitudes of the two electrometric responses. From the data it is obvious that the amplitudes of the electrometric responses are the same. This shows that both transitions are electrogenic to the same extent and consequently should be associated with the same amount of transferred charge. In **III** we also demonstrate that this mutant is capable of proton pumping. This means that the electrogenicity observed in the electrometric experiments is not due to the chemistry of the enzyme and both $\mathbf{P_R}$→**F** and $\mathbf{P_M}$→**F** transitions are associated with the same amount of proton pumping.

5.1.5 Complete single turnover

The complete catalytic cycle of cytochrome *c* oxidase consists of two parts - reductive and oxidative. During the reductive phase the oxidized enzyme receives electrons from cytochrome *c*. In order to comply with electroneutrality, protons enter cytochrome *c* oxidase at the same time in order to compensate the charge. In the oxidative phase the reduced enzyme reacts with oxygen. This part of the reaction includes the high-potential intermediates **P** and **F**, which are capable of proton pumping (Wikström, 1989; Wikström and Morgan, 1992). The

electrometric flow-flash data discussed above (**I**, **II**, **III**) gives us information about the electrogenicity only during the oxidative part of the reaction. However, the amount of charges transferred during the complete single turnover – oxidative plus reductive phases – can also be ascertained using the electrometric method.

We have measured the development of electric potential starting from the fully reduced CO-bound enzyme in the presence of an excess of CO and a very low concentration of oxygen (**IV**). After photolysis of the enzyme-CO complex, only a small fraction of the enzyme (in our experiment only ~2%) reacts with oxygen and enters the oxidative phase (**IV**, Fig. 3a); the majority recombines with CO. The enzyme fraction that is oxidized may be re-reduced immediately at a rate that depends on the concentration of reduced cytochrome *c* present in the sample as a reductant. After reduction, most of this fraction recombines with CO. Although 2% of it may again react with the oxygen present, this represents only 0.04% of the total enzyme and can be neglected. Therefore, this experimental arrangement allows time-resolved measurement of charge translocation during a complete single cycle of enzyme oxidation and re-reduction (**IV**, Fig. 3a). Special care was taken to ensure that full re-reduction of the enzyme occurred at the highest cytochrome *c* concentrations employed.

As it is shown in **IV**, Fig. 3b the response indeed consists of two phases. The rate of the first phase does not depend on the reductant concentration and represents the oxidative part of the reaction. Increasing the concentration of reductant (traces 1-4), increases the rate and apparent extent of the slower reductive phase to its maximum, where its amplitude accounts for 56.3% (±3.01 s.d; 7 independent experiments) of the overall charge translocation. Of the charges, 43.7% cross the membrane during the fast oxidative phase, which is distinguished by the fact that its amplitude is independent of the cytochrome *c* concentration, but varies with the CO concentration in the sample. The full electrogenesis – vectorial chemistry plus proton pumping – during the complete single turnover of cytochrome *c* oxidase – oxidative plus reductive phases – is in total eight electrical charges (**IV**, Fig. 1b, c). From this electrometric experiment it follows that the oxidative and reductive phases contribute to the total by 3.5 charges during the oxidative and 4.5 charges during the reductive phases.

In **IV** we directly measured the amount of pumping during a single turnover of bovine cytochrome *c* oxidase using a pH electrode. Simultaneous to the pH response we followed the absorbance of hemes *a* and a_3 at 445-470 nm (**IV**, Fig. 2). When the sample was anaerobic and fully reduced, as judged by the optical assay, but with no additional reductant present, there is a release of only about 2 protons (**IV**, Fig. 2a), in agreement with earlier data (Oliveberg *et al.*, 1991). The absorbance trace of the lower panel confirms that the entire enzyme population is rapidly oxidized. In contrast, when oxidation is followed by immediate re-reduction, a total of four protons are ejected owing to complete proton pumping (**IV**, Fig. 2b). Full reduction of the enzyme is not necessary in order to achieve ejection of four protons, which occurs already after about 40% reduction of the two heme groups, the redox states of which are followed in the lower trace of **IV**, Fig. 2b. On the other hand, reduction of the enzyme in state **O**, without a preceding oxidative phase, does not lead to significant proton release (data not shown). Thus, proton pumping is incomplete for both the oxidative and reductive phases when assayed alone, and translocation of four protons occurs only if oxidation is immediately followed by re-reduction.

Half of the eight charges translocated per oxygen molecule reduced are due to the electrical events associated with proton pumping (Wikström, 1977; Babcock and Wikström, 1992). We conclude (**IV**) that when the reduced enzyme is oxidized by dioxygen and immediately re-reduced, about two electrical charges are translocated owing to proton pumping events in each phase. The simplified interpretation of the earlier thermodynamic data (Wikström, 1989), that all proton translocation takes place during the oxidative phase, is thus erroneous. However, our data also show that proton translocation is not coupled energetically to the reductive phase, as has been proposed (Michel, 1998; Capitanio *et al.*, 2000), because in that

case it should occur during enzyme reduction without prior oxidation. As proton pumping occurs only when immediately preceded by an oxidative phase, all the energy for proton translocation may indeed be conserved during the oxidative phase (Wikström, 1989). Half of this energy is converted into electrogenic proton movement across the dielectric during oxidation, but the other half must be conserved in the enzyme species preceding **O** (**IV**, Fig 1a), which is the product of the oxidative phase. This energy is released for proton translocation only if the enzyme receives electrons immediately; otherwise it is lost as heat.

A primary result from our work (**IV**) is the idea that energy from the redox processes in the oxidative phase of the catalytic cycle can be conserved in a meta-stable state of the enzyme. The bimetallic heme-copper center is in the ferric/cuppric form (Wikström, 1989; Babcock and Wikström, 1992) in state **O**. Our results thus indicate that there may be two forms of this state, **O** and **H**, of which **H** is the immediate product of the oxidative phase with energy conserved for proton translocation (**IV**, Fig. 6).

5.2 Electron backflow in cytochrome *c* oxidase

During the reaction with oxygen cytochrome *c* oxidase couples the electron transfer inside the protein to the proton translocation across the phospholipid membrane. This electron transfer in the enzyme is called the forward flow of electrons. In cytochrome *c* oxidase there is another observable electron transfer process called backflow. It is not observed during the normal course of the reaction with oxygen, but it is very useful for studying the electron transfer phenomenon in this enzyme. In the binuclear site CO binds to heme a_3 and significantly raises its midpoint potential, stabilizing the electron on the metal center. The heme a_3-CO bond is photolabile and can be destroyed by a short flash of light. When the partially reduced CO-bound enzyme is photolyzed in the absence of oxygen electrons redistribute in the enzyme (Boelens and Wever, 1979; Boelens *et al.*, 1982; Brzezinski and Malmström, 1987; Morgan *et al.*, 1989; Oliveberg and Malmström, 1991; Verkhovsky *et al.*, 1992; Georgiadis *et al.*, 1994). After photolysis of CO the midpoint potential of heme a_3 drops to its original value and electron from heme a_3 flow backwards in the enzyme and tend to distribute between all four redox centers – heme *a*, heme a_3, Cu_A and Cu_B – till it reaches the redox equilibrium. This final equilibrium is determined by the redox potentials of the cofactors and interactions between them.

In a brief outline, the backflow process consists of a series of equilibrium states: the CO molecule dissociates from heme a_3 instantly (in a few hundreds of femtoseconds, which is the first vibration of heme a_3-CO bond) but before leaving the enzyme it transiently binds to the Cu_B (Woodruff *et al.*, 1991; Einarsdóttir *et al.*, 1993). As it is discussed above (section 2.3) the fastest reported electron transfer event from heme a_3 to heme *a* happens with a time constant of 3 μs (Oliveberg and Malmström, 1991). In the next phase, as a slower event, electrons distribute from heme *a* to Cu_A (Morgan *et al.*, 1989; Verkhovsky *et al.*, 1992). This process has a characteristic time constant about 50-70 μs. The final equilibrium, after the photolysis of carbon monoxide, is reached on a millisecond time scale and it is caused by the dissociation and backward diffusion of the internally bound proton(s) (Hallén *et al.*, 1994), which were preloaded during the reduction of the binuclear site (Mitchell and Rich, 1994).

5.2.1 Electrometric backflow

The electron transfer from heme *a* to Cu_A is coupled to the vectorial transfer of charge across the membrane and this process should be detectable using the electrometric method. As it is demonstrated in **I**, the backflow process can be observed using the electrometric setup. Here it appears as a positive signal in contrast to the flow-flash response, which in our experimental

setup has a negative sign. This indicates that the response is associated with the movement of negative charge from heme *a* upwards in the membrane to Cu_A. The same polarity of the electrometric response would be associated with the movement of a positively charged proton in the other direction.

The amount of electron backflow between hemes is maximal at the two-electron reduction level, or at the mixed-valence state. At this reduction level the electron transfer to Cu_A is very small and makes-up only 1-2%. As it is discussed in **I**, the dark titration model, the extent of additional reduction of Cu_A increases with the reduction of enzyme and reaches its maximal amplitude at the three-electron reduction level. Such a behavior is a direct consequence of the redox interactions between redox centers. By reducing the enzyme further the extent of Cu_A reduction after CO photolysis starts to decrease and becomes zero at the fully reduced state. So, after all, there is a characteristic bell shape redox potential behavior of the amplitude of additional electron transfer to Cu_A after CO photolysis. The extent of reduction of the enzyme in the sample can also be controlled by using different mediators and a redox buffer in the medium (**I**). Such a behavior is shown as circles in **I**, Fig. 6.

The amplitude of the backflow response is quite small. Even at its maximum, the bell shaped plot of Cu_A reduction versus initial redox state of the enzyme is usually in the order of 0.2-0.8 mV. The number of kinetic components in such a response is quite large and the signal to noise ratio of a single trace is not good enough to resolve so many components. In order to improve the signal to noise ratio of the response we tried two approaches. First we used averaging of the signal. In the electrometric setup we used the glucose/catalase/glucose oxidase system which keeps the sample anaerobic and also slowly reduces the enzyme. The speed of reduction of the enzyme was slow enough to average every 50 traces. In order to achieve better separation of the kinetic components we combined all electrometric traces – from mixed-valence to fully reduced – into a single surface and analyzed this surface at once using a multiexponential fitting program. As some later phases of the backflow process are quite slow, in these experiments we used a 1% carbon monoxide mixture with 99% of argon. In this case the relaxation of the signal (the CO recombination) does not influence the amplitude of the slowest phases.

The global fit of the data surface resolves three major electrogenic phases during the development of $\Delta\psi$ and two components of CO binding. CO recombination is different in the mixed-valence and fully-reduced states of the enzyme, which is in agreement with (Morgan *et al.*, 1993). In addition to these phases, in the very beginning of the response there is a very fast electrogenic phase with a time constant of 1-2 μs. The amplitude of this phase increases with the reduction of the enzyme and is maximal at the fully reduced state. This phase titrates with the reduction of heme *a*.

According to the results of the multiexponential fit, the first electrogenic process after the CO photolysis has a time constant of 66 μs. Usually, in order to assign electrometric processes, we have to use the optical absorption technique. The same time constant was detected optically after the photolysis of CO from the mixed-valence state and was assigned to the electron transfer from heme *a* to Cu_A (Oliveberg *et al.*, 1991; Verkhovsky *et al.*, 1992) (**I**, Fig. 5). This phase has a maximum amplitude at the three electron state, which is in agreement with the assignment and as it is predicted by theoretical model in **I**, the dark titration model for the electron transfer from heme *a* to Cu_A.

According to the optical data (see above) the 66 μs phase is the second electron equilibration after photolysis of carbon monoxide. During the first equilibrium, an electron is transferred between the hemes. This process has a time constant of 3 μs (Oliveberg and Malmström, 1991). The fact that this process is not observed in the electrometric response indicates that electron transfer between the hemes is exactly in parallel to the membrane plane. Even a small deviation from this route would raise quite a large electrogenic signal, because the

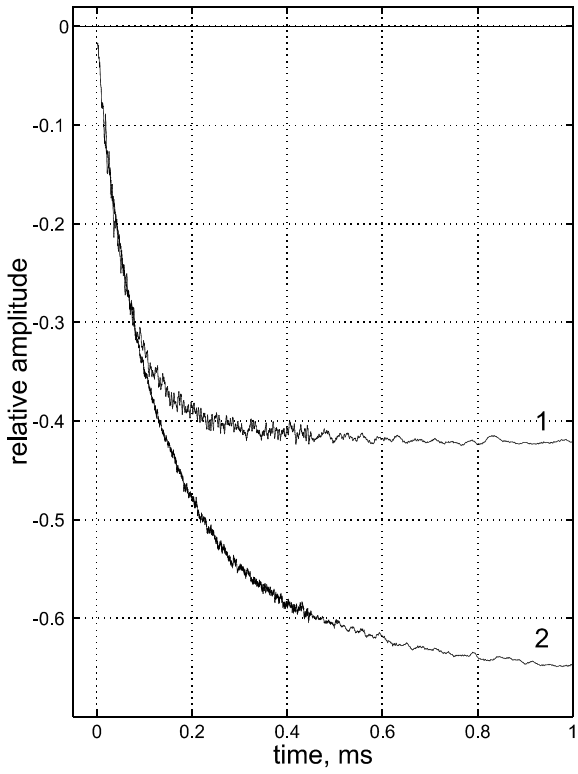

Figure 4. The comparison between optical kinetic at 820 nm (trace 1) and electrometric response (trace 2) after CO photolysis. In both cases the enzyme was three-electron reduced.

extent of this electron transfer is in the order of 50%. This result gives very important information when modeling a phospholipid membrane around the enzyme's crystallographic structure.

In order to assign the 66 µs phase more firmly we have directly measured optical absorbance changes at 820 nm where Cu_A absorbs maximally. Indeed, the additional reduction of Cu_A after the photolysis of CO is very small at the mixed-valence reduction level. It increases with the reduction of the enzyme, reaches a maximum at the three-electron level and disappears in the fully-reduced enzyme (data not shown). The analysis of the trace of the three-electron reduced enzyme shows that there is a single component with a time constant ~60 µs. On the other hand the electrometric trace at the same reduction level clearly consists of two components with time constants 66 µs and 300 µs (Fig. 4). This clearly demonstrates that only the 66 µs phase is associated with the electrogenic electron transfer to Cu_A.

5.2.2 Ultra fast heme-heme electron transfer

As it was discussed in the previous chapter, the backflow process is a cascade of equilibriums. After the photodissociation of CO from the reduced active site of the enzyme, the first electron distributes between the hemes. In the next, slower step, the electron redistributes between all three redox centers: heme a_3, heme a and Cu_A. Even later, protons start to leave the binuclear site and this again causes additional electron re-equilibration. Using the system with CO present in the sample it is very difficult to reach the final equilibrium of electrons and protons, because carbon monoxide starts to inhibit the process. The last equilibrium is achieved very slowly and in the electrometric method the relaxation of the measuring membrane complicates the final state even further.

We applied conventional optical absorption spectroscopy in order to study the final equilibrium which the two electron enzyme approaches after the complete removal of CO. In order to achieve that task we formed the mixed-valence state of the enzyme where only two electrons are present in the enzyme and are bound by CO in the binuclear center. Then, in order to remove the bound carbon monoxide, the sample was purged with argon and after a few repetitions the carbon monoxide was completely removed. In this case, there is equilibration of only one electron. If initially there are only two electrons the electron distributes only between

hemes and the amount transferred to Cu_A is insignificant (see **I**, dark titration model). The difference spectrum between the final spectrum after removal of CO and the mixed-valence spectrum before removal of CO shows the final equilibrium state of the enzyme. We decomposed this difference spectrum using the spectra of both hemes and the CO binding spectrum as a basis set. Using this approach we can determine the total amount of electrons which were transferred during this process.

The data from one analysis is shown in **V**, Fig. 2C. The spectral decomposition of the difference spectrum shows that at the final electron equilibrium a total of 50-60% of electrons are transferred from heme a_3 to heme *a* after total removal of CO from mixed-valence state of the enzyme.

In order to determine during which time span this electron transfer occurs we have measured optically the kinetics of fast electron transfer. According to our data the first observable electron transfer between hemes happens with a time constant of 3 µs which is in good agreement with the literature (Oliveberg and Malmström, 1991; Verkhovsky *et al.*, 1992). The amount of this electron transfer monotonically decreases with the reduction of the enzyme and is maximal at the mixed-valence state. According to our calculations only 20-25% of heme a_3 oxidizes during this process and it is the only process where a significant amount of heme a_3 oxidizes at the studied pH 7. So the question is where is the rest of the electron transfer?

V, Fig. 2A demonstrates the results of an optical experiment where we monitored CO photolysis from the mixed-valence state of the enzyme. We used a 1% CO concentration in order to prevent CO binding as long as possible and very intensive measuring light, which would immediately photolyze any CO molecules which bound to the enzyme. The time resolution of the spectrophotometer used in this experiment is 1 ms. During the first millisecond the distribution of an electron reaches equilibrium. The difference between the final spectrum and spectrum before the photolysis is shown in **V**, Fig. 2A where it is compared with the spectrum discussed above. It is clear that these spectra are identical and proves that we are reaching the final equilibrium in the CO photolysis experiment. The absence of additional slower phases indicates that the "missing" electron transfer should happen faster than 3 µs.

We compared the optical kinetics at 605 nm for the mixed-valence and fully reduced enzyme in the same sample (**V**, Fig. 3). Since the amplitude of the photolysis should be the same in both states of the reduction (the extinction of the process should not change) it is clear from the figure that there is an additional phase after the photolysis which is not resolved in our setup. The optical kinetic spectrum of this phase is the same as the 3 µs phase. This shows that after CO photolysis the electron transfer from heme a_3 to heme *a* happens in two phases. The 3 µs phase is the second part and the amount of electron transferred in the first part is about 25-30%.

The present experimental setup does not allow us to resolve this phase in time, but it is possible to add some constraints. As it is shown in **V**, the spectrum of the unresolved phase is the same as 3 µs phase and demonstrates the electron transfer from heme a_3 and heme *a*. The time constant of this phase has to be faster than 40 ns, because there is no such a phase in (Einarsdóttir *et al.*, 1992), where the time resolution was 40 ns.

It is well known that biological electron transfer reactions may be limited by coupling to protonation or ligand changes, and such limitations have also been described for cytochrome *c* oxidase (Verkhovsky *et al.*, 1995). However, the 3 µs phase of heme-heme electron transfer is insensitive to changes in pH and to substituting D_2O for H_2O (Oliveberg and Malmström, 1991; Hallén *et al.*, 1994). The lack of pH and deuterium isotope effects on the electron transfer rate indicates that this phase is strictly due to electron tunneling (Brzezinski, 1996; Regan *et al.*, 1998; Medvedev *et al.*, 2000). Very recently, Cherepanov *et al.*, (2001) described two kinetically distinct phases of biological electron transfer, where the fast phase is due to nonadiabatic electron tunneling whereas the slow phase is limited by protein relaxation. The

contribution of the latter becomes prominent at low driving forces, where $-\Delta G_0$ approaches Λ, the energy of protein relaxation. For the present case, where the amplitude of the fast tunneling event accounts for more than one half of the combined two phases (**V**, Fig. 3 and 4B) and ΔG_0 is –26 meV, we can estimate that Λ is of the order of 30 meV. Hence, the 3 μs electron transfer phase may be limited by relaxation of the complex between the heme cofactors and the protein.

In conclusion, electron transfer between the heme groups of cytochrome *c* oxidase is divided into two kinetically very different phases; previously unnoted fast electron tunneling at a rate of $\geq 10^8\ s^{-1}$, and the well-known electron equilibration at $3 \cdot 10^5\ s^{-1}$. The sum of their amplitudes is consistent with the total extent of electron transfer observed at equilibrium. The rate of the fast phase is consistent with the theory of Dutton (Page *et al.*, 1999), which at an average protein packing density, ΔG_0 = -26 meV, a reorganization energy of 0.7 eV, and using the shortest distance between the aromatic heme systems (7.3 Å), predicts a rate of $6 \cdot 10^8\ s^{-1}$. The slower phase of electron transfer may be limited by heme/protein relaxation (Cherepanov *et al.*, 2001). It seems clear from these results that electron transfer between the two heme groups in cytochrome *c* oxidase cannot itself limit or control catalysis. Instead, it is tuned to be very fast by the close apposition of the hemes, which in turn guarantees effective kinetic trapping of an oxygen molecule (Chance *et al.*, 1975; Verkhovsky *et al.*, 1996).

The nature of such a split of electron transfer between hemes is not clear at the time, but some predictions are possible. The electron transfer is very fast between the hemes, on a sub-nanosecond time scale. The 3 μs phase of electron transfer could be observable as it is modulated by some kind of ligand exchange in the binuclear site under the oxidation of heme a_3. The possible candidate for such a ligand is carbon monoxide. After photolysis from heme a_3 the CO molecule transiently binds to Cu_B (Woodruff *et al.*, 1991). This process occurs with a time constant of 1.5 μs in the fully-reduced enzyme. It is possible that in the mixed-valence state this process is a little bit slower – 3 μs. In such a case the oxidation of heme a_3 would be modulated by the dissociation of CO from Cu_B.

5.3 Proton pumping during different parts of the cycle.

The electrometric signal, during the reaction of the fully reduced cytochrome *c* oxidase with dioxygen, has a very good signal to noise ratio and is very informative about the rates of the processes. It shows which steps in the reaction are coupled to the charge translocation across the membrane and it is possible to compare the electrogenicities of different phases. Unfortunately, the electrometric signal itself does not indicate how many charges are transferred in a particular step in the reaction. To determine how many millivolts correspond to the movement of one charge all the way across the membrane requires independent evaluation; monitoring other electrogenic process where the amount of transferred charges is known.

The backflow process, which was discussed in the previous section, is a good candidate for such a calibration. The fast phase of the electrometrically observed backflow is associated with the vectorial transfer of an electron from heme *a* to Cu_A. In the previous section it was shown that this phase is coupled to pure electron transfer and no protons are involved (see above). The amplitude of this phase has a maximum at the three-electron reduction level of the enzyme.

We used optical spectroscopy in order to estimate the amount of electron transfer to Cu_A (**I**). Using this method it is possible to tell exactly the amount of additional reduction of Cu_A during the backflow process at the maximum (three-electron reduction) level. In the paper we used the whole response at 605 nm and 445 nm and calculated that 12.5% of Cu_A was reduced by heme *a*. In this calibration we included the middle phase (see above) of the backflow process, which was later found not to be associated with electron transfer to Cu_A. The same was also true

for the electrometrical signal – the calculations were based on the entire amplitude of the backflow. Recently, we measured optically the kinetics at 820 nm where Cu_A absorbs maximally (Fig. 4, trace 1). The results showed only one additional phase of reduction of Cu_A after photolysis of CO. This phase has a time constant of ~60 μs. Using the optical kinetics at 445 nm and 605 nm and taking into account only the 60 μs phase we found that about 7.3% of Cu_A is reduced by heme *a* at the three-electron reduction level.

When we know exactly how many electrons are transferred to Cu_A during the backflow, we can recalibrate the electrometric signal. The fast phase of the electrometrically observed backflow is associated with pure electron transfer to Cu_A. In one of the samples, according to the fit, the maximal amplitude of this phase is 0.31 mV. If we assume that the whole dielectric distance across the membrane is equal to unity and the dielectric distance from Cu_A to the heme *a* level inside the membrane equals **d**, then for the electrometric backflow process in the fast phase we can write the equation:

$$0.073\varphi\mathbf{d} = 0.31 \text{ mV}$$

where φ is the amplitude of the electrometric signal when one charge is transferred across the whole dielectric.

Let us now quantitate the electrometric signal when the fully reduced cytochrome *c* oxidase reacts with dioxygen (the oxidative part of the cycle). For the same sample as above, the amplitude of the flow-flash electrometric signal is 57 mV. For this we can write the equation:

$$\mathbf{n}\varphi = 57 \text{ mV}$$

where **n** is the number of charges transferred across the membrane during the oxidative part of the cycle. So there is one more unknown, which should be obtained independently from another experiment.

The data from the complete single turnover experiments show that the ratio between the oxidative and reductive parts of the electrometric signal is 0.78 (**V**). In addition to that, it is firmly established that a total of 8 charges are transferred across the lipid bilayer during the complete cycle of cytochrome *c* oxidase. From these data we can calculate how many charges are transferred in each part of the cycle separately. We can write the set of equations:

$$\begin{cases} \mathbf{n}/\mathbf{m} = 0.78 \\ \mathbf{n} + \mathbf{m} = 8 \end{cases}$$

where **n** is the number of charges in the oxidative part of the cycle and **m** is the same number in the reductive part. By solving this latter set of equations we conclude that in the oxidative part there are 3.51 charges transferred and in the reductive part 4.49 charges are transferred across the dielectric bilayer.

Combining all these equations into one set:

$$\begin{cases} 0.073\varphi\mathbf{d} = 0.31\text{mV} \\ \mathbf{n}\varphi = 57\text{mV} \\ \mathbf{n}/\mathbf{m} = 0.78 \\ \mathbf{n} + \mathbf{m} = 8 \end{cases}$$

And solving this set of equations we determine these very important constants:

$$\mathbf{d} = 0.26,\ \mathbf{n} = 3.51,\ \mathbf{m} = 4.49 \text{ and } \varphi = 16.24 \text{ mV}$$

The value of dielectric distance **d** calculated here is smaller than 0.5 (Hinkle and Mitchell, 1970). The difference between the algorithm used previously and presently is due to two different experimental approaches – results of the electrometric flow-flash and the complete single turnover, which are more precise. In addition, during the procedure the amount of electron transfer to Cu_A was evaluated more precisely. The lower value of the dielectric distance fits better with the crystallographic data. According to the structure, the geometric distance from the surface of the membrane to heme *a* iron level in the membrane is about 0.3. Also, the area above both hemes contains many water molecules. The crystallographically defined water molecules can be considered firmly bound in the protein structure, therefore not part of the common water pool. Still, the presence of water in the surrounding dielectric will increase the macroscopic dielectric constant locally and consequently lower the dielectric distance **d**. The value 0.26 in this case is quite acceptable.

Using the calculated value for **d** we can make some other calculations. During the complete reduction of the enzyme approximately 2.4 protons are taken up by the enzyme, two of which are associated exclusively with the reduction of the binuclear site (Mitchell and Rich, 1994). In other words, in the fully reduced enzyme there are two protons already preloaded close to the binuclear site. Those charges will be electronically silent during the reaction with oxygen. During the full catalytic cycle of cytochrome *c* oxidase four chemical protons are used. Those two missing protons will be preloaded during the reaction with oxygen. Since these protons are taken-up from the N-side of the membrane, electrogenically they have to cross 1-**d** dielectric distance. Also, from the electrogenical point of view, during the chemical cycle, one electron will be transferred from Cu_A to the binuclear site and must cross the dielectric distance **d**. Together, this will result in

$$2\cdot(1-\mathbf{d}) + \mathbf{d} = 1.74.$$

This number is the contribution of the vectorial chemistry the total electrogenicity during the oxidative part of the reaction. The total number of charges transferred during the oxidative part is **n** = 3.51. The difference between these two numbers gives us the amount of proton pumping during the oxidative part of the cycle, which is 1.77 charges (protons). According to the electrometric flow-flash data (**I**) there are two major electrogenic phases during the oxidative part of the catalytic cycle. The amplitudes of those two phases are equal. As it is discussed in **I**, these phases represent the **P→F** and **F→O** transitions. Since the electrometric amplitudes of those phases are equal, 0.89 charges are transferred across the total dielectric during each of those transitions. Considering that there is no other charge movement during the oxidative phase of the reaction with oxygen, we conclude that one proton is being pumped during each of the **P→F** and **F→O** transitions. It should also be noted that the evaluation of the dielectric distance **d** is extremely sensitive to changes in the other parameters.

5.4 Conclusions

The discussed electrometric experiments gives us valuable information about which parts of the catalytic cycle of cytochrome *c* oxidase are coupled with charge translocation, information which can not be obtained by any other experimental technique. Using time-resolved electrometry it is possible to study charge movements inside the enzyme which are ultimately coupled to the transitions between intermediates during the reaction of the enzyme with oxygen

with a microsecond time resolution (**I**, **II**, **III**). With the same time resolution, it is also possible to study the fast electron and proton electrogenic transfer reactions during the backflow process (**I**, **II**, **V**). Under some particular conditions, the electrometric method enables us to follow the development of electrogenic reactions during the complete single turnover of the enzyme (**IV**). It is possible to do these experiments using the same sample. With a combination of optical absorption spectroscopy and electrometric methods it is possible to calibrate the electrometric signal, which itself is not quantitative.

The main conclusion of paper **IV** is that proton translocation by bovine cytochrome *c* oxidase is not solely coupled to the oxidative part of the reaction as was previously thought (Wikström, 1989). On the opposite hand, half of the proton pumping happens during the reductive part of the cycle if the enzyme is reduced shortly after oxidation. In order to explain these results we introduced the hypothetical intermediate **H** into the cycle (Fig. 5), which spontaneously decays into the oxidized state **O** if the enzyme is not reduced. The transition of **H**→**R** *via* the **O** intermediate is not coupled with proton pumping, only the preloading of protons into the oxidase. Contrary, the straight transition **H**→**R** is associated with large scale proton and electron transfer, pumping of two protons and uptake of two protons upon the reduction of the binuclear site. This interpretation may still be compatible with previous data (Wikström, 1989; Wikström and Morgan, 1992). It is clear that the greatest amount of energy is released during the oxidative part of the reaction, which involves high potential oxygen intermediates. The energy could be released during the oxidative part of the chemical cycle, but the actual act of storing the energy – proton pumping – could be realized later in the cycle.

The division of the proton pumping equally between the oxidative and reductive portions of the cycle has another implication. The electrometric response during the oxidative half of the

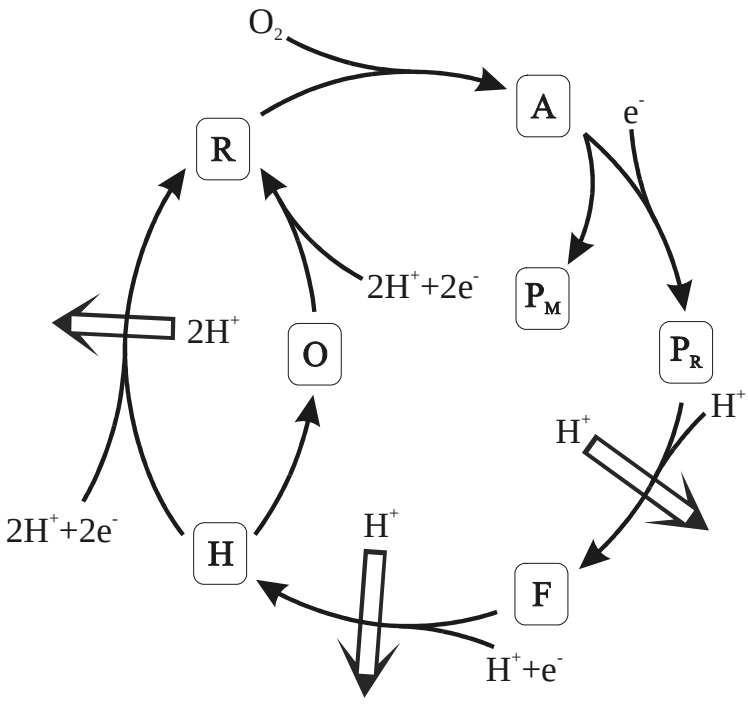

Figure 5. The proposed model of the catalytic cycle.

reaction shows that equal amounts of the electric charge are translocated across the lipid membrane during the **P→F** and **F→O** transitions (**I**). The evaluation of the amount of actual charge shows that about one proton is being pumped in each of these transitions. The electrometric studies of the oxygen reaction in the R54M mutant form of cytochrome *c* oxidase from *P. denitrificans* shows that both $\mathbf{P_M}\rightarrow\mathbf{F}$ and $\mathbf{P_R}\rightarrow\mathbf{F}$ transitions are electrogenic to the same extent. This in turn clearly demonstrates that the $\mathbf{P_M}\rightarrow\mathbf{F}$ transition (not shown in Fig. 5) is also coupled to the pumping of one proton across the membrane. This statement challenges the model of proton pumping proposed by the Frankfurt group (Michel, 1998; Michel, 1999).

Summary

In this work the catalytic function of cytochrome *c* oxidase was studied using the electrometric technique. This method allows direct, real time measurements of the electric charge movements across the phospholipid membrane during the catalytic turnover. A sub-microsecond time resolution of this method was achieved to measure the very fast, partial steps in the reaction of cytochrome *c* oxidase with oxygen. The most important outcome of using this method is the knowledge as to which parts of the catalytic cycle are connected to electrogenicity and proton pumping.

The catalytic cycle of cytochrome *c* oxidase consists of two parts – oxidative and reductive. The oxidative part, during which the reduced enzyme reacts with oxygen, exhibits two electrogenic phases. These electrogenic reactions are coupled to the **P→F** and **F→O** transitions and the amount of electrogenicity in these steps is equal.

In this work an experimental methodology was developed which allows electrometric measurements of the full catalytic cycle of cytochrome *c* oxidase – oxidation plus reduction. Surprisingly, the results showed that the oxidative phase, which is coupled to the formation and decay of higher potential intermediates, is not coupled to the largest part of electrogenicity. The amount of transferred charges is even larger during the reductive part of the cycle.

The electron backflow process in the partially reduced enzyme is another electrogenic reaction in cytochrome *c* oxidase. By combining optical spectroscopy with the electrometric method, it is possible to calibrate the internal electron transfer between redox centers during different parts of the cycle. It was determined that the oxidative and reductive parts of the catalytic cycle are each coupled to pumping of two protons, but not all four protons, during the oxidative phase. Taking into account the flow-flash data we conclude that the **P→F** and **F→O** transitions are coupled to pumping of one proton each.

Acknowledgements

The present work was started in the Division of Medical Chemistry, Dept. of Biomedical Sciences (Biolääketieteen laitos), Medical Faculty and finished in the Department of Biosciences, Division of Biochemistry, Faculty of Sciences of the University of Helsinki and it was carried out in the Helsinki Bioenergetics Group. It was started in December 1996 when I was still studying at Vilnius University in Lithuania.

I wish to express my deep gratitude to the leader of the Helsinki Bioenergetis Group Professor Mårten Wikström for accepting me to the group and providing excellent experimental conditions and free working atmosphere.

My deepest thanks go to my teachers (supervisors) here in Helsinki – Professor Michael Verkhovsky and Dr. Joel Morgan – who supported and inspired me in the field of Bioenergetics. Thank you very much for your patience and endless energy. I will never forget those long discussions about oxidase with Misha and Joel thanks to which I learned something in the field. Special thanks to Joel for the first and the largest lead to the Unix world. I will also never forget days and nights spent doing the beef heart prep.

The reviewers of this manuscript, Professor Ilmo Hassinen and Professor Robert Gennis, are acknowledged for their constructive criticism and valuable suggestions.

I am deeply grateful to my co-authors, especially to Camilla Backgren, Marina Verkhovskaya, Vitaliy Borisov and Alexander Konstantinov. I wish to thank Ilja Belevich and Markus Kaukonen for sharing the office space with me. I owe my special thanks to Anne Tuukkanen who I have been sharing the electrometric setup for collegial support and always good mood.

I wish to thank all the past and present members of the Helsinki Bioenergetics Group for warm and friendly working environment. Special thanks to Monday Meetings which made us always have some new results. I would like to especially express my gratitude to Pamela David for being a friend and an excelent english teacher. Thank you very much for revising english language in the manuscript.

I would like to express my special thanks to group's secretary Satu Sankkila for her help and care all the time from my first minutes in Finland. Her great guidance and help were and are felt all the time. Thank you very much for letting me know finish customs and traditions.

Dr. Nikolai Belevich I want to thank for his excellent technical help and computer knowledge.

Above all, my warmest thanks go to my wife Agne for her love, patience and support sharing these laborious years with me. Her love and presence have enriched my life enormously.

Finally, I would like to thank my parents Antanas Jasaitis and Danute Jasaitiene for their unconditional love throughout my life and the support which they gave me during all that long time of my education years.

Financial support was provided by grants from the Center for International Mobility (CIMO), the Academy of Finland, the University of Helsinki and Biocentrum Helsinki.

Helsinki, January 2002

Audrius Jasaitis

References

Abramson, J., Riistama, S., Larsson, G., Jasaitis, A., Svensson-Ek, M., Laakkonen, L., Puustinen, A., Iwata, S. and Wikström, M. (2000) *Nature Struct. Biol.*, **7**, 910-917.

Antalis, T.M. and Palmer, G. (1982) *J. Biol. Chem.*, **257**, 6194-6206.

Antholine, W.E., Kastrau, D.H.W., Steffens, G.C.M., Buse, G., Zumft, W.G. and Kroneck, P.M.H. (1992) *Eur. J. Biochem.*, **209**, 875-881.

Antonini, E., Brunori, M., Colosimo, A., Greenwood, C. and Wilson, M.T. (1977) *Proc. Natl. Acad. Sci. U.S.A.*, **74**, 3128-3132.

Babcock, G.T. and Callahan, P.M. (1983) *Biochem.*, **22**, 2314-2319.

Babcock, G.T., Callahan, P.M., Ondrias, M.R. and Salmeen, I. (1981) *Biochemistry*, **20**, 959-966.

Babcock, G.T., Varotsis, C. and Zhang, Y. (1992) *Biochim. Biophys. Acta*, **1101**, 192-194.

Babcock, G.T., Vickery, G.T. and Palmer, G. (1976) *J. Biol. Chem.*, **251**, 7901-7919.

Babcock, G.T. and Wikström, M. (1992) *Nature*, **356**, 301-309.

Baker, G.M., Noguchi, M. and Palmer, G. (1987) *J. Biol. Chem.*, **262**, 595-604.

Beinert, H., Hansen, R.E. and Hartzell, C.R. (1976) *Biochim. Biophys. Acta*, **423**, 339-355.

Beinert, H. and Shaw, R.W. (1977) *Biochim. Biophys. Acta*, **462**, 121-130.

Blackmore, R.S., Greenwood, C. and Gibson, Q.H. (1991) *J. Biol. Chem.*, **266**, 19245-19249.

Blair, D.F., Witt, S.N. and Chan, S.I. (1985) *J. Am. Chem. Soc.*, **107**, 7389-7399.

Blomberg, M.R.A., Siegbahn, P.E.M., Babcock, G.T. and Wikström, M. (2000) *J. Am. Chem. Soc.*, **122**, 12848-12858.

Boelens, R. and Wever, R. (1979) *Biochim. Biophys. Acta*, **547**, 296-310.

Boelens, R., Wever, R. and Van Gelder, B.F. (1982) *Biochim. Biophys. Acta*, **682**, 264-272.

Borisov, V., Gennis, R. and Konstantinov, A.A. (1995) *Biochem. Mol. Biol. Int.*, **37**, 975-982.

Brown, S., Rumbley, J.N., Moody, A.J., Thomas, J.W., Gennis, R.B. and Rich, P.R. (1994) *Biochim. Biophys. Acta*, **1183**, 521-532.

Brudvig, G.W., Stevens, T.H., Morse, R.H. and Chan, S.I. (1981) *Biochemistry*, **20**, 3912-3921.

Brunori, M., Antonini, G., Malatesta, F., Sarti, P. and Wilson, M.T. (1987) *Eur. J. Biochem.*, **169**, 1-8.

Brzezinski, P. (1996) *Biochemistry*, **35**, 5611-5615.

Brzezinski, P. and Malmström, B.G. (1987) *Biochim. Biophys. Acta*, **894**, 29-38.

Buse, G., Soulimane, T., Dewor, M., Meyer, H.E. and Bloggel, M. (1999) *Prot. Sci.*, **8**, 985-990.

Calhoun, M.W., Thomas, J.W. and Gennis, R.B. (1994) *TIBS*, **19**, 325-330.

Capaldi, R.A. (1990) *Annu. Rev. Biochem.*, **59**, 569-596.

Capitanio, N., Capitanio, G., Boffoli, D. and Papa, S. (2000) *Biochemistry*, **39**, 15454-15461.

Carter, K. and Palmer, G. (1982) *J. Biol. Chem.*, **257**, 13507-13514.

Casey, R.P., Chappell, J.B. and Azzi, A. (1979) *Biochem. J.*, **182**, 149-156.

Chan, S.I. and Li, P.M. (1990) *Biochemistry*, **29**, 1-12.

Chance, B., Saronio, C. and Leigh, J.S., Jr. (1975) *J. Biol. Chem.*, **250**, 9226-9237.

Chen, Y.-R., Gunther, M.R. and Mason, R.P. (1999) *J. Biol. Chem.*, **274**, 3308-3314.

Cherepanov, D.A., Krishtalik, L.I. and Mulkidjanian, A.Y. (2001) *Biophys. J.*, **80**, 1033-1049.

Clore, M.G., Andreasson, L.-E., Karlsson, B.G., Aasa, R. and Malmstrom, B. (1980) *Biochem. J.*, **185**, 139-154.

Cooper, C.E. and Salerno, J.C. (1992) *J. Biol. Chem.*, **267**, 280-285.

Drachev, L.A., Jasaitis, A.A., Kaulen, A.D., Kondrashin, A.A., Liberman, E.A., Nemecek, I.B., Ostroumov, S.A., Semenov, A.Y. and Skulachev, V.P. (1974) *Nature*, **249**, 321-324.

Drachev, L.A., Kaulen, A.D. and Skulachev, V.P. (1978) *FEBS Lett.*, **87**, 161-167.

Dyer, R.B., Einarsdóttir, O., Killough, P.M., López-Garriga, J.J. and Woodruff, W.H. (1989) *J. Am. Chem. Soc. 1989*, **111**, 7651-7659.

Dyer, R.B., Peterson, K.A., Stoutland, P.O. and Woodruff, W.H. (1991) *J. Am. Chem. Soc.*, **113**, 6276-6277.

Dyer, R.B., Peterson, K.A., Stoutland, P.O. and Woodruff, W.H. (1994) *Biochemistry*, **33**, 500-507.

Eglinton, D.G., Hill, B.C., Greenwood, C. and Thomson, A.J. (1984) *J. Inorg. Biochem.*, **21**, 1-8.

Einarsdóttir, O., Dawes, T.D. and Georgiadis, K.E. (1992) *Proc. Natl. Acad. Sci. USA*, **89**, 6934-6937.

Einarsdóttir, O., Dyer, R.B., Lemon, D.D., Killough, P.M., Hubig, S.M., Atherton, S.J., Lopez-Garriga, J.J., Palmer, G. and Woodruff, W.H. (1993) *Biochemistry*, **32**, 12013-12024.
Einarsdóttir, O., Georgiadis, K.E. and Sucheta, A. (1995) *Biochemistry*, **34**, 496-508.
Fabian, M. and Palmer, G. (1995) *Biochemistry*, **34**, 13802-13810.
Fabian, M., Wong, W.W., Gennis, R.B. and Palmer, G. (1999) *Proc. Natl. Acad. Sci. U.S.A.*, **96**, 13114-13117.
Fann, Y.C., Ahmed, I., Blackburn, N.J., Boswell, J.S., Verkhovskaya, M.L., Hoffman, B.M. and Wikström, M. (1995) *Biochemistry*, **34**, 10245-10255.
Ferguson-Miller, S. and Babcock, G.T. (1996) *Chem. Rev.*, **7**, 2889-2907.
Fetter, J.R., Qian, J., Shapleigh, J., Thomas, J.W., Garcia-Horsman, A., Schmidt, E., Hosler, J., Babcock, G.T., Gennis, R.B., *et al.* (1995) *Proc. Natl. Acad. Sci. USA*, **92**, 1604-1608.
Garcia-Horsman, J.A., Barquera, B., Rumbley, J., Ma, J. and Gennis, R.B. (1994) *J. Bacteriol.*, **176**, 5587-5600.
Garcia-Horsman, J.A., Puustinen, A., Gennis, R.B. and Wikström, M. (1995) *Biochemistry*, **34**, 4428-4433.
Georgiadis, K.e., Jhon, N.-I. and Einarsdóttir, O. (1994) *Biochemistry*, **33**, 9245-9256.
Geren, L.M., Beasley, J.R., Fine, B.R., J., S.A., Hibdon, S., Pielak, G.J., Durham, B. and Millet, F. (1995) *J. Biol. Chem*, **270**, 2466-2472.
Gibson, Q.H. and Greenwood, C. (1963) *Biochem. J.*, **86**, 541-554.
Goldbeck, R.A., Dawes, T.D., Einarsdóttir, O., Woodruff, W.H. and Kliger, D.S. (1991) *Biophys. J.*, **60**, 125-134.
Goldbeck, R.A., Einarsdottir, O., Dawes, T.D., O'Connor, D.B., Surerus, K.K., Fee, J. and Kliger, D.S. (1992) *Biochemistry*, **31**, 9376-9387.
Gray, H.B. and Winkler, H.B. (1996) *Ann. Rev. Biochem.*, **65**, 537-561.
Gray, K.A., Grooms, M., Myllykallio, H., Moomaw, C., Slaughter, C. and Daldal, F. (1994) *Biochemistry*, **33**, 3120-3127.
Greenaway, F.T., Chan, S.H.P. and Vincow, G. (1977) *Biochim. Biophys. Acta*, **490**, 62-78.
Greenwood, G. and Gibson, Q.H. (1967) *J. Biol. Chem.*, **242**, 1782-1787.
Hallén, S., Brzezinski, P. and Malmström, B.G. (1994) *Biochemistry*, **33**, 1467-1472.
Hallén, S. and Nilsson, T. (1992) *Biochemistry*, **31**, 11853-11859.
Hallén, S., Svensson, M. and Nilsson, T. (1993) *FEBS. Lett.*, **325**, 299-302.
Han, S., Ching, Y.-C. and Rousseau, D.L. (1990) *Proc. Natl. Acad. Sci. USA*, **87**, 2491-2495.
Hanson, D.K., Tiede, D.M., Nance, S.L., Chang, C.-H. and Schiffer, M. (1993) *Proc. Natl. Acad. Sci. U.S.A.*, **90**, 8929-8933.
Hansson, Ö., Karlsson, B., Aasa, R., Vängård, T. and Malmström, B.G. (1982) *EMBO J.*, **1**, 1295-1297.
Hellwig, P., Grzybek, S., Behr, J., Ludwig, B., Michel, H. and Mäntele, W. (1999) *Biochemistry*, **38**, 1685-1694.
Hill, B.C. (1991) *J. Biol. Chem.*, **266**, 2219-2226.
Hill, B.C. and Greenwood, C. (1983) *Biochem. J.*, **215**, 659-667.
Hill, B.C. and Greenwood, C. (1984) *Biochem. J.*, **218**, 913-921.
Hill, B.C., Greenwood, C. and Nicholls, P. (1986) *Biochim. Biophys. Acta*, **853**, 91-113.
Hill, B.C., Hill, J.J. and Gennis, R.B. (1994) *Biochemistry*, **33**, 15110-15115.
Hill, B.H. (1994) *J. Biol. Chem.*, **269**, 2419-2425.
Hinkle, P. and Mitchell, P. (1970) *Bioenergetics*, **1**, 45-60.
Hosler, J.P., Ferguson-Miller, S., Calhoun, M.W., Thomas, J.W., Hill, J., Lemieux, L., Ma, J., Georgiou, C., Fetter, J., *et al.* (1993) *J. Bioenerg. Biomembr.*, **25**, 121-136.
Iwata, S., Ostermeier, C., Ludwig, B. and Michel, H. (1995) *Nature*, **376**, 660-669.
Junemann, S. (1997) *Biochim. Biophys. Acta*, **1321**, 107-127.
Kadenbach, B. (1986) *J. Bioenerg. Biomembr.*, **18**, 39-54.
Kahlow, M.A., Zuberi, T.M., Gennis, R.B. and Loehr, T.M. (1991) *Biochemistry*, **30**, 11485-11489.
Kannt, A., Pfitzner, U., Ruitenberg, M., Hellwig, P., Ludwig, B., Mantele, W., Fendler, K. and Michel, H. (1999) *Journal of Biological Chemistry*, **274**, 37974-81.
Karlsson, B., Aasa, R., Vängård, T. and Malmström, B.G. (1981) *FEBS Lett.*, **131**, 186-188.
Karlsson, B. and Andréasson, L.-E. (1981) *Biochim. Biophys. Acta*, **635**, 73-80.

Kelly, M., Lappalainen, P., Talbo, G., Haltia, T., van der Oost, J. and Saraste, M. (1993) *J. Biol. Chem.*, **268**, 16781-16787.
Kobayashi, K., Une, H. and Hayashi, K. (1989) *J. Biol.Chem.*, **246**, 7976-7980.
Konstantinov, A.A., Siletskiy, S.A., Mitchell, D., Kaulen, A.D. and Gennis, R.B. (1997) *Proc. Natl. Acad. Sci. U.S.A.*, **94**, 9085-9090.
Krab, K. and Wikström, M. (1978) *Biochim. Biophys. Acta*, **504**, 200-214.
Kuhn-Neutwig, L. and Kadenbach, B. (1985) *Eur. J. Biochem.*, **149**, 147-158.
Lappalainen, P., Aasa, R., Malmström, B.G. and Saraste, M. (1993) *J. Biol. Chem.*, **268**, 26416-26421.
Lauraeus, M., Morgan, J.E. and Wikström, M. (1993) *Biochemistry*, **32**, 2664-2670.
Lorence, R.M. and Gennis, R.B. (1989) *J. Biol. Chem.*, **264**, 7135-7140.
Lübben, M., Kolmer, B. and Saraste, M. (1992) *EMBO J.*, **11**, 805-812.
MacMillan, F., Kannt, A., Behr, J., Prisner, T. and Michel, H. (1999) *Biochemistry*, **38**, 9179-9184.
Malmström, B.G. and Aasa, R. (1993) *FEBS Lett.*, **325**, 49-52.
Medvedev, D.M., Daizadeh, I. and Stuchebrukhov, A.A. (2000) *J. Am. Chem. Soc.*, **122**, 6571-6582.
Michel, H. (1998) *Proc.Natl. Acad. Sci U.S.A.*, **95**, 12819-12824.
Michel, H. (1999) *Biochemistry*, **38**, 15129-15140.
Michel, H., Behr, J., Harrenga, A. and Kannt, A. (1998) *Annu. Rev. Biophys. Biomol. Struct.*, **27**, 329-356.
Miller, M.J. and Gennis, R.B. (1985) *J. Biol. Chem.*, **260**, 14003-14008.
Mitchell, P. (1961) *Nature*, **191**, 141-148.
Mitchell, P. (1988) *Ann. N.Y. Acad. Sci.*, **550**, 185-198.
Mitchell, R., Mitchell, P. and Rich, P.R. (1991) *FEBS Lett.*, **280**, 321-324.
Mitchell, R., Mitchell, P. and Rich, P.R. (1992) *Biochim. Biophys. Acta*, **1101**, 188-191.
Mitchell, R. and Rich, P.R. (1994) *Biochim. Biophys. Acta*, **1186**, 19-26.
Moody, A.J., Cooper, C.E. and Rich, P.R. (1991) *Biochim. Biophys. Acta*, **1059**, 189-207.
Morgan, J.E., Blair, D.F. and Chan, S.I. (1985) *J. Inorg. Biochem.*, **23**, 295-302.
Morgan, J.E., Li, M.P., Jang, D.-J., El-Sayed, M.A. and Chan, S.I. (1989) *Biochemistry*, **28**, 6975-6983.
Morgan, J.E., Verkhovsky, M.I., Palmer, G. and Wikström, M. (2001) *Biochemistry*, **40**, 6882-6892.
Morgan, J.E., Verkhovsky, M.I., Puustinen, A. and Wikström, M. (1995) *Biochemistry*, **34**, 15633-15637.
Morgan, J.E., Verkhovsky, M.I., Puustinen, A.e. and Wikström, M. (1993) *Biochemistry*, **32**, 11413-11418.
Morgan, J.E., Verkhovsky, M.I. and Wikstrom, M. (1996) *Biochemistry*, **35**, 12235-12240.
Morgan, J.E., Verkhovsky, M.I. and Wikström, M. (1994) *J. Bioenerg. Biomembr.*, **26**, 599-608.
Moser, C.C., Keske, J.M., Warncke, K., Farid, R.S. and Dutton, P.L. (1992) *Nature*, **355**, 796-802.
Nilsson, T. (1992) *Proc. Natl. Acad. Sci. U.S.A.*, **89**, 6497-6501.
Ogura, T., Takahashi, S., Hirota, S., Shinzawa-Itoh, K., Yoshikawa, S., Appelman, E.H. and Kitagawa, T. (1993) *J. Am. Chem. Soc.*, **115**, 8527-8536.
Ogura, T., Takahashi, S., Shinzawa-Itoh, K., Yoshikawa, S. and Kitagawa, T. (1990) *J. Biol. Chem.*, **265**, 14721-14723.
Oliveberg, M., Brzezinski, P. and Malmström, B.G. (1989) *Biochem. Biophys. Acta*, **977**, 322-328.
Oliveberg, M., Hallén, S. and Nilsson, T. (1991) *Biochemistry*, **30**, 436-440.
Oliveberg, M. and Malmström, B.G. (1991) *Biochemistry*, **30**, 7053-7057.
Oliveberg, M. and Malmström, B.G. (1992) *Biochemistry*, **31**, 3560-3563.
Orii, Y. (1988) *Ann. NY Acad. Sci.*, **550**, 105-117.
Ostermeier, C., Harrenga, A., Ermler, U. and Michel, H. (1997) *Proc. Natl.Acad.Sci. USA*, **94**, 10547-10553.
Page, C.C., Moser, C.C., Chen, X. and Dutton, P.L. (1999) *Nature*, **402**, 47-52.
Platt, J.R. (1956) in *Radiation Biology* (Hollander, A. Eds.), pp. 71-121, McGraw-Hill Book Company, Inc., New York.
Proshlyakov, D.A., Ogura, T., Shinzawa-Itoh, K., Yoshikawa, S. and Kitagawa, T. (1996) *Biochemistry*, **35**, 76-82.
Proshlyakov, D.A., Pressler, M.A. and Babcock, G.T. (1998) *Proc. Natl. Acad.Sci. U.S.A.*, **95**, 8020-8025.
Proshlyakov, D.A., Pressler, M.A., DeMaso, C., Leykam, J.F., DeWitt, D.L. and Babcock, G.T. (2000) *Science*, **290**, 1588-1591.

Puustinen, A., Finel, M., Haltia, T., Gennis, R.B. and Wikström, M. (1991) *Biochemistry*, **30**, 3936-3942.
Puustinen, A., Verkhovsky, M.I., Morgan, J.E., Belevich, N.P. and Wikström, M. (1996) *Proc. Natl. Acad. Sci. U.S.A.*, **93**.
Puustinen, A. and Wikström, M. (1991) *Proc. Natl. Acad. Sci. U.S.A.*, **88**, 6122-6126.
Raitio, M. and Wikström, M. (1994) *Biochim. Biophys. Acta*, **1186**, 100-106.
Regan, J.J., Ramirez, B.E., Winkler, J.R., Gray, H.B. and Malmström, B.G. (1998) *J. Bioenerg. Biomembr.*, **30**, 35-48.
Rieder, R. and Bosshard, H.R. (1980) *J. Biol. Chem.*, **255**, 4732-4739.
Riistama, S. (2000) Ph.D. Thesis. Helsinki University, Helsinki.
Riistama, S., Laakkonen, L., Wikstrom, M., Verkhovsky, M.I. and Puustinen, A. (1999) *Biochemistry*, **38**, 10670-10677.
Riistama, S., Puustinen, A., Verkhovsky, M.I., Morgan, J.E. and Wikstrom, M. (2000) *Biochemistry*, **39**, 6365-72.
Riistama, S., Verkhovsky, M.I., Laakkonen, L., Wikstrom, M. and Puustinen, A. (2000) *Biochim Biophys Acta*, **1456**, 1-4.
Rousseau, D.L., Ching, Y.-c. and Wang, J. (1993) *J. Bioenerg. Biomemb.*, **25**, 165-176.
Ruitenberg, M., Kannt, A., Bamberg, E., Ludwig, B., Michel, H. and Fendler, K. (2000) *Proc. Natl. Acad. Sci. U.S.A.*, **97**, 4632-6.
Saraste, M. (1990) *Q. Rev. Biophys.*, **23**, 331-366.
Siletsky, S., Soulimane, T., Azarkina, N., Vygodina, T.V., Buse, G., Kaulen, A. and Konstantinov, A. (1999) *FEBS Letters*, **457**, 98-102.
Soulimane, T., Than, M.E., Dewor, M., Huber, R. and Buse, G. (2000) *Protein Science*, **9**, 2068-2073.
Steffens, G.C.M., Soulimane, T., Wolff, G. and Buse, G. (1993) *Eur. J. Biochem.*, **213**, 1149-1157.
Stoutland, P., Lambry, J.-C., Martin, J.-L. and Woodruff, W.H. (1991) *J. Phys. Chem.*, **95**, 6406-6408.
Sucheta, A., Szundi, I. and Einarsdottir, O. (1998) *Biochemistry*, **37**, 17905-17914.
Thomas, J.W., Puustinen, A., Alben, J.O., Gennis, R.B. and Wikström, M. (1993) *Biochemistry*, **32**, 10923-10928.
Tsukihara, T., Aoyama, H., Yamashita, E., Takashi, T., Yamaguichi, H., Shinzawa-Itoh, K., Nakashima, R., Yaono, R. and Yoshikawa, S. (1996) *Science*, **272**, 1136-1144.
van der Oost, J., Pappalainen, P., Musacchio, A., Warne, A., Lemieux, L., Rumbley, J., Gennis, R.B., Aasa, R., Pascher, T., *et al.* (1992) *EMBO J.*, **11**, 3209-3217.
Varotsis, C. and Babcock, G.T. (1990) *Biochemistry*, **29**, 7357-7362.
Varotsis, C., Woodruff, W.H. and Babcock, G.T. (1989) *J. Am. Chem. Soc.*, **111**, 6439-6440.
Varotsis, C., Zhang, Y., Appelman, E.H. and Babcock, G.T. (1993) *Proc. Natl. Acad. Sci. U.S.A.*, **90**, 237-241.
Verkhovsky, M.I., Morgan, J.E., Puustinen, A. and Wikström, M. (1996) *Nature*, **380**, 268-270.
Verkhovsky, M.I., Morgan, J.E., Verkhovskaya, M. and Wikstrom, M. (1997) *Biochim. Biophys. Acta*, **1318**, 6-10.
Verkhovsky, M.I., Morgan, J.E. and Wikström, M. (1992) *Biochemistry*, **31**, 11860-11863.
Verkhovsky, M.I., Morgan, J.E. and Wikström, M. (1994) *Biochemistry*, **33**, 3079-3086.
Verkhovsky, M.I., Morgan, J.E. and Wikström, M. (1995) *Biochemistry*, **34**, 7483-7491.
Verkhovsky, M.I., Tuukkanen, A., Backgren, C., Puustinen, A. and Wikström, M. (2001) *Biochemistry*, **40**, 7077-7083.
Vygodina, T. and Konstantinov, A. (1989) *Biochim. Biophys. Acta*, **973**, 390-398.
Weng, L. and Baker, G.M. (1991) *Biochemistry*, **30**, 5727-5733.
Wikström, M. (1977) *Nature*, **266**, 271-273.
Wikström, M. (1981) *Proc. Natl. Acad. Sci. U.S.A.*, **78**, 4051-4054.
Wikström, M. (1989) *Nature*, **338**, 776-778.
Wikström, M. (2000) *Biochim. Biophys. Acta*, **1458**, 188-198.
Wikström, M., Jasaitis, A., Backgren, C., Puustinen, A. and Verkhovsky, M.I. (2000) *Biochim. Biophys. Acta*, **1459**, 514-520.
Wikström, M. and Morgan, J.E. (1992) *J. Biol. Chem.*, **267**, 10266-10273.
Wikström, M.K.F. (1972) *Biochim. Biophys. Acta*, **283**, 358-390.
Wikström, M.K.F. and Saari, H.T. (1977) *Biochim. Biophys. Acta*, **462**, 347-361.

Wikström, M.K.F. and Saris, N.E.L. (1970) in *Electron Transport and Energy Conservation* (Tager, J.M., Papa, S., Quagliariello, E. and Slater, E.C. Eds.), pp. 77-88, Adriatica Editrice, Bari.

Wilks, A. and Ortiz de Montellano, P.R. (1992) *J. Biol. Chem.*, **267**, 8827-8833.

Wilmanns, M., Lappalainen, P., Kelly, M., Sauer-Eriksson, E. and Saraste, M. (1995) *Biochemistry*, **92**, 11955-11959.

Winkler, J.R., Malmström, B.G. and Gray, H.B. (1995) *Biophys. Chem.*, **54**, 199-209.

Witt, D.N. and Chan, S.I. (1987) *J. Biol. Chem.*, **262**, 1446-1448.

Witt, H. and Ludwig, B. (1997) *J. Biol. Chem.*, **272**, 5514-5517.

Woodruff, W.H. (1993) *J. Bioenerg. Biomemb.*, **25**, 177-188.

Woodruff, W.H. and Dyer, R.B. (1993) in *Biological Spectroscopy, Part B* (Clark, R.J.H. and Hester, R.E. Eds.), pp. 189-233, John Wiley Press, Chichester, PA.

Woodruff, W.H., Einarsdottir, O., Dyer, R.B., Bagley, K.A., Palmer, G., Atherton, S.J., Goldbeck, R.A., Dawes, T.D. and Kliger, D.S. (1991) *Proc. Natl. Acad. Sci. U.S.A.*, **88**, 2588-2592.

Wrigglesworth, J. (1984) *Biochem. J.*, **217**, 715-719.

Wrigglesworth, J.M., Elsden, J., Chapman, A., Van der Water, N. and Grahn, M.F. (1988) *Biochim. Biophys. Acta*, **93**, 452-464.

Wu, W., Chang, C.K., Varotsis, C., Babcock, G.T., Puustinen, A. and Wikström, M. (1992) *J. Am. Chem. Soc.*, **114**, 1182-1187.

Yanamura, W., Zhang, Y.Z., Takamiya, A. and Capaldi, R.A. (1988) *Biochemistry*, **27**, 4909-4914.

Yoshikawa, S., Shinzawa-Itoh, K., Nakashima, R., Yaono, R., Inoue, N., Yao, M., Fei, M.J., Libeu, C.P., Mizushima, T., *et al.* (1998) *Science*, **280**, 1723-1729.

Zaslavsky, D., Kaulen, A., Smirnova, I.A., Vygodina, T.V. and Konstantinov, A.A. (1993) *FEBS Lett.*, **336**, 389-393.

Zimmermann, B.H., Nitsche, C.I., Fee, J.A., Rusnak, F. and Münck, E. (1988) *Proc. Natl. Acad. Sci. U.S.A.*, **85**, 5779-5783.